Stony Brook University

OFFICIAL COPY

The official electronic file of this thesis or dissertation is maintained by the University Libraries on behalf of The Graduate School at Stony Brook University.

© All Rights Reserved by Author.

X-ray reflectivity studies on polystyrene dead layers

A Thesis Presented

By

Chen Liang

To

The Graduate School

In Partial Fulfillment of the

Requirements

For the Degree of

Master of Science

In

Materials Science and Engineering

Stony Brook University

May 2012

Stony Brook University

The Graduate School

Chen Liang

We, the thesis committee for the above candidate for the
Master of Science degree, hereby recommend
acceptance of this thesis.

Tadanori Koga --- Thesis Adviser
Assistant Professor, Department of Materials Science and Engineering

Jonathon Sokolov --- Committee Member
Professor, Department of Materials Science and Engineering

Michael Dudley --- Committee Member
Professor, Department of Materials Science and Engineering

This thesis is accepted by the Graduate School

Charles Taber
Interim Dean of the Graduate School

Abstract of the Thesis

X-ray reflectivity studies on polystyrene dead layers

A Thesis Presented

By

Chen Liang
Master of Science
in
Materials Science and Engineering
Stony Brook University
2012

This thesis mainly focuses on the novel characters of the adsorbed layers formed at the solid substrate by using in-situ x-ray reflectivity. We characterized the thermal expansion as a function of temperature. We found the contraction of the adsorbed layer within the T-range from room temperature to 100℃, which is in contrast to the bulk behavior. We also found that the heterogeneous structure in the direction normal to the surface: the bulk-like top layer and high density bottom layer.

Table of Contents

List of Figures v

List of Tables vii

Acknowledgments viii

Chapter 1 Introduction 1

1.1 Background and Motivation 1

1.1.1 Polystyrene 1

1.1.2 Glass transition temperature 2

1.1.3 Dead layer 3

1.1.4 Thermal expansivity 3

1.1.5 Ellipsometry 4

1.1.6 X-ray reflectivity 5

1.1.7 Atomic Force Microscopy 7

Chapter 2 Review of the Literature 9

2.1 Glass transition temperature (T_g) behavior of polymer thin film study 9

2.2 Thermal expansion behavior (α) of polymer thin film study 10

2.3 Roughness behavior of polymer thin film study 11

2.4 Annealing effects on thickness of polystyrene thin film 11

2.5 Substrate effect on polymer thin film 11

Chapter 3 Materials and Methods 13

3.1 Solution Preparation 13

3.2 Substrate Preparation 13

3.3 Spin-cast films 14

3.4 Sample Annealing 14

3.5 Washing by Toluene 14

3.6 Ellipsometry 15

3.7 X-ray Reflectivity 15

3.8 Atomic Force Microscopy 15

Chapter 4 Experiment Results and Discussion 16

1st Experiment --- Thickness of adsorbed layers depends on the annealing time. 16

2nd Experiment --- Dead layer 22

3rd Experiment --- Study the molecular mobility of PS adsorbed layers 23

4th Experiment --- X-ray reflectivity results for PS 4nm, 9nm and 50nm 25

Chapter 5 Conclusion 41

References 42

List of Figures

Figure 1. Polystyrene formation 2
Figure 2. Adsorbed layer formation process 3
Figure 3. Schematic setup of an ellipsometry. 4
Figure 4. X-ray instrument from Brookhaven Laboratory 5
Figure 5. Reflectivity Geometry. 6
Figure 6. Interpretation of x-ray data 7
Figure 7. a) Spring depiction of cantilever. b) SEM image of triangular SPM cantilever with probe (tip). 7
Figure 8. Process and data for the experiment of PS (M_w=290K, C=2.5wt%). 16
Figure 9. Thickness of adsorbed layer from ellipsometry vs annealing hours 17
Figure 10. Specular reflectivity profiles and their corresponding modeled fits (solid lines) measured for polystyrene films (290K 2.5wt%) with varying annealing time. 18
Figure 11. Thickness and delta of adsorbed layer PS (M_w=290K, C=2.5wt%) vs annealing time. 19
Figure 12. Process and data for the experiment of PS (M_w=290K, C=0.2wt%). 19
Figure 13. Specular reflectivity profiles and their corresponding modeled fits (solid lines) measured for polystyrene film (M_w=290K, C=0.2wt%) with varying temperature. 20
Figure 14. Thickness and delta of adsorbed layer PS (M_w=290K, C=0.2wt%) vs annealing time. 21
Figure 15: Delta and thickness vs annealing time by different concentration. 21
Figure 16. Process and data of the second experiment. 22
Figure 17. Thickness of adsorbed layer vs days immerse in toluene in air condition. 23
Figure 18. Procedure used for the third experiment. 23
Figure 19. Procedure and data used for the third experiment. 24
Figure 20. Specular reflectivity profiles and their corresponding modeled fits (solid lines) measured for PS (4nm in thickness, 90℃ for 1h annealed) in air with varying temperature. 25
Figure 21. Thickness and delta for PS (4nm in thickness, 90℃ -1h annealed) vs temperature, measured in the air. 26
Figure 22. Specular reflectivity profiles and their corresponding modeled fits (solid lines) measured for PS (4nm in thickness, 150℃ for 24h annealed) in air with varying temperature. 27
Figure 23. Thickness and delta of PS (4nm in thickness, 150℃ -24h annealed) vs temperature, measured in the air. 28
Figure 24: AFM image for PS (M_w= 290K, 4nm in thickness, 150℃ -24h annealed) 30
Figure 25. Specular reflectivity profiles and their corresponding modeled fits (solid lines) measured for PS (4nm in thickness, 150℃ for 24h annealed) under vacuum with varying temperature. 31
Figure 26. Thickness and delta of PS (M_w=290K, 4nm in thickness, 150℃-24h annealed) vs. temperature under vacuum. 32
Figure 27: AFM image for PS (M_w=290K, 4nm in thickness, annealed 150℃ for 24h, measured under vacuum) 33

Figure 28. An ultrathin polystyrene film was annealed and then heated incrementally to 80℃, cooled, and then reheated to 80℃. The first heating cycle are showed as black dots, and the second heating cycle are showed as write dots. [16] 34
Figure 29. Temperature dependence of thickness of weakly annealed (left) and strongly annealed (right) deuterated polystyrene thin films with various values of initial thickness. For the strongly annealed experiment, measurements were done in heating and cooling process. [15] 35
Figure 30. Specular reflectivity profiles and their corresponding modeled fits (solid lines) measured for PS (9nm in thickness, 150℃ for 24h annealed) with increasing temperature under vacuum 36
Figure 31. Thickness and delta for PS (M_w=290K, 9nm in thickness, 150°C-24h annealing) vs. temperature, measuring under vacuum. 37
Figure 32. Specular reflectivity profiles and their corresponding modeled fits (solid lines) measured for PS (50nm in thickness, 150℃ for 24h annealed) under vacuum with varying temperature. 38
Figure 33. Thickness of bottom and top layer vs. Temperature. 39
Figure 34. Total thickness vs. temperature. 39
Figure 35. Delta for the bottom and top layer vs. temperature respectively. 40

List of Tables

Table 1. Calculated thickness and delta for PS (M_w=290K, 2.5wt%) with different annealing time. 18

Table 2. Calculated thickness and delta for PS (M_w=290K, C=0.2wt%) with different annealing time. 20

Table 3. Thickness, delta and roughness for PS (4nm in thickness, 90℃ for 1h annealed) with increasing temperature in air. Data was fitted by three layer model. 26

Table 4. Thickness, delta and roughness for PS (4nm in thickness, 150℃ for 24h annealed) with increasing temperature in air. 28

Table 5. Thickness, delta and roughness for PS (4nm in thickness, 150℃ for 24h annealed) with increasing temperature under vacuum. 31

Table 6. Data compared at 30℃ before and after experiment. 33

Table 7. Thickness, delta and roughness for PS (9nm in thickness, 150℃ for 24h annealed) with increasing temperature under vacuum. 36

Table 8. Thickness, delta and roughness for PS (50nm in thickness, 150℃ for 24h annealed) with increasing temperature in air condition. 38

Acknowledgments

First, I would like to express my sincere gratitude to Professor Tadanori Koga, my academic advisor, for his excellent guidance and constant support during these years. Without his instructions and ideas this thesis cannot be finished.

The support of my senior Naisheng Jiang and Peter Gin are greatly appreciated. I am very grateful for their support and constructive comments. Especially, Naisheng Jiang sent me to BNL several times, taught me how to use X-ray reflectivity and fit data.

Many thanks to all the members in Koga's group. It is really a joy to work with her during my graduate studies. I truly feel blessed to have such a wonderful group.

At last but not least, this thesis is dedicated to my dear parents, Fulin Liang and He Chen, for their unconditional support and love.

Chapter 1 Introduction

1.1 Background and Motivation

Nowadays, nanotechnology intends to produce functional nanosize devices which demand stable, homogeneous, and uniform polymer films at the nanometer scale. This demand is driving widespread studies on polymer thin films more than a couple of decades. Knowledge of many material properties, from coefficient of thermal expansion to dielectric constant, is crucial for better device design, simulation, and performance. Polymer thin films are omnipresent in electronics as packaging materials, which are increasingly being investigated for use in active chip component applications [1]. Those polymer thin films show unusual characteristics such as abnormal film thickness dependence of glass transition temperature (T_g) [2-5] and thermal expansivity [6, 7]. They also demonstrate large annealing effects and ultraslow relaxation in their glass and molten states [7, 8].

Several different studies have been investigated on T_g and thermal expansion of polymer thin films supported on silicon substrates as a function of initial film thickness. It was found that polymer thin film (the thickness less than several hundred angstroms) can have properties very different from the bulk and related to many other important phenomena such as wetting, adhesive, surface friction, and glass transition temperature. Thus, polymer thin films studies are important from viewpoints of not only academic but also industrial application.

1.1.1 Polystyrene

Polystyrene (PS) is an aromatic polymer made of the monomer styrene, which is produced from petroleum by the chemical industry. It is a long chain hydrocarbon wherein alternating carbon centers are attached to phenyl group. The chemical formula for polystyrene is $(C_8H_8)_n$. There are short range van der Waals attractions between polymers chains. The intermolecular weakness confers elasticity and flexibility. Because the molecules are long hydrocarbon chains which contains thousands of atoms, the total attractive force exist between the molecules is huge. The

chains are hardly broken, but take on a higher degree of conformation and slide each other when heated.

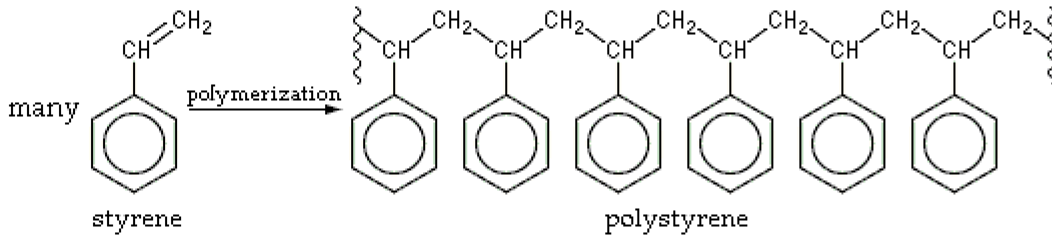

Figure 1. Polystyrene formation

It is an inexpensive and hard plastic, and probably PS is one of the most widely used in our everyday life. From outside housing of the computer we are using everyday, to the clear plastic drinking cups; from Cars and airplane, to foam packaging are all could be made from PS.

PS can either be a thermoset or a thermoplastic material. It is in a solid state at room temperature, but flows when the temperature above T_g = 100°C, and become solid after cooling down. The melting temperature T_m is always higher than T_g, about 240°C for PS. Pure solid PS is hard plastic with limited flexibility and colorless, but it can be transparent or can be made to take on various colors.

1.1.2 Glass transition temperature

Glass transition is a reversible transition in amorphous materials or in amorphous regions within semicrystalline materials from a hard and relatively brittle state to a molten or rubbery state. T_g of polymer thin films is also one of the most interesting phenomena because many properties such as thermal and mechanical properties change remarkably at T_g. When the temperature higher than T_g, amorphous macromolecular materials are rubbery, viscous fluids, however, when the temperature lower than T_g, they are showed as glassy and more or less brittle.

Extensive studies have been carried out to what degree the surface and interfacial T_g's of polymeric materials vary relative to the bulk values, with the motivation being their important

role in different applications such as disk drive lubricants, membranes, nanocomposites, photoresists, and biomaterials. In order to design highly functionalized polymeric materials and understand the physical properties at surface and interfacial regions, which are impossible to deduce via extrapolate simply from the bulk parameters, is of great significance. It was widely recognized that T_g is directly related to the thermal stability of polymer thin films. Aiming to explain the special nature of T_g of polymer thin film and/or surface, many studies have been carried on with various methods, including ellipsometry, x-ray reflectivity, neutron reflectometry, positron annihilation, birllouin light scattering, dielectric relaxtion, and atomic force microscopy so far.

1.1.3 Dead layer

Scientists recently found that a very thin polymer layer at the substrate interface with an attractive substrate usually showed as regions with almost null expansion coefficients and absence of molecular mobility. Because of these extreme characteristics, the layer is considered as "dead" layers. Being a direct reflection of changes in the system properties in the approach to the interface, the dead layer is a general issue of the reduction or enhancement of the material's performance on the nano-scale rather than a specific feature of polymer thin films.

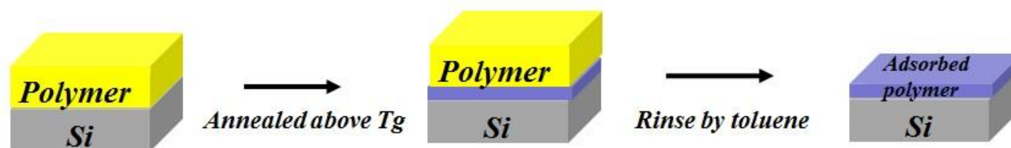

Figure 2. Adsorbed layer formation process

1.1.4 Thermal expansivity

Thermal expansion widely exists in Mother Nature, which is the tendency of matter to change in volume in response to change in temperature. When a substance is heated, its particles begin moving more than before and usually maintain a greater average separation. Most materials

expand with increasing temperature. The degree of expansion divided by the change in temperature is called a coefficient of thermal expansion and generally varies with temperature.

The thermal expansion of the total thickness should be calculated from the average of each layer, which is given by:

$$\alpha_g = \frac{1}{D}\sum_i \alpha_{g,i} d_i, \quad \alpha_l = \frac{1}{D}\sum_i \alpha_{l,i} d_i, \quad D = \sum_i d_i,$$

D and d_i are the total film thickness and the film thickness of each layer.
Where $a_{g,i}$ and $a_{l,i}$ are the thermal expansivity of i-th layer in the glass state and the molten state, respectively. Using the observed a_g and a_l, we can calculate the total thickness of a_g and a_l.

1.1.5 Ellipsometry

Ellipsometry is an optical technique I used to measure the thickness of polymer thin films in my experiments. It has many applications in different areas, from semiconductor physics to microelectronics, from basic laboratory research to industrial applications.

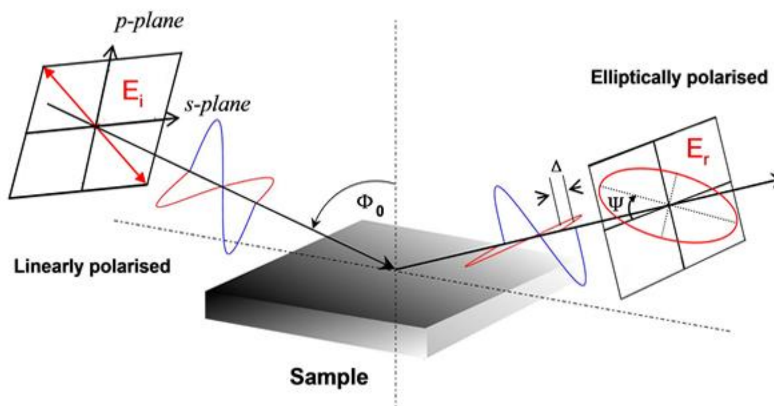

Figure 3. Schematic setup of an ellipsometry.

Ellipsometry only measures the change of polarization during reflection or transmission. Usually, ellipsometry is done only in the reflection setup. Sample's properties, such as thickness, complex

refractive index or dielectric function tensor, determine the exact nature of polarization change. Even though the optical techniques are diffraction limited inherently, ellipsometry take advantages of phase information and the polarization state of light, and can reach angstrom resolution.

1.1.6 X-ray reflectivity

X-ray reflectivity is a surface-sensitive analytical technique used in physics, chemistry, and materials science, which is able to provide accurate thickness values for both thin films and multilayers with high accuracy, as well as density, roughness of surface and interface.

Figure 4. X-ray instrument from Brookhaven Laboratory

The basic notion for this technique is to measure the intensity of x-rays reflected from a flat surface with the specular condition which the reflected angle equal to incident angle. If the interface is not smooth, the reflected intensity will deviate from that predicted by the law of Fresnel reflectivity. The deviations can be analyzed to obtain the graph of density from the surface normal to the interface. In order to determine the thickness and roughness with high accuracy, it is necessary to precisely align a sample position to the X-ray beam. All the alignment process is controlled by a computer. What we should do is to put a sample on a

vertical sample stage, which is installed on a higher resolution goniometer under vacuum or in air. The angular resolution of the instrument 2θ is 0.0002^{o}. Adjusting the position of z and ω (or θ) repeatedly, an optimum position is letting the sample located at the center of the X-ray beam line and only half of the X-beam line can be detected by the detector. After that, by setting the detector (2θ) in an appropriate position, the total external reflection adjustment will start after open the beam line.

Figure 5 shows the reflectivity geometry for the x-ray reflectivity. The incoming beam reflects form the surface and interface of each layer at an angle equal to the incident angle.

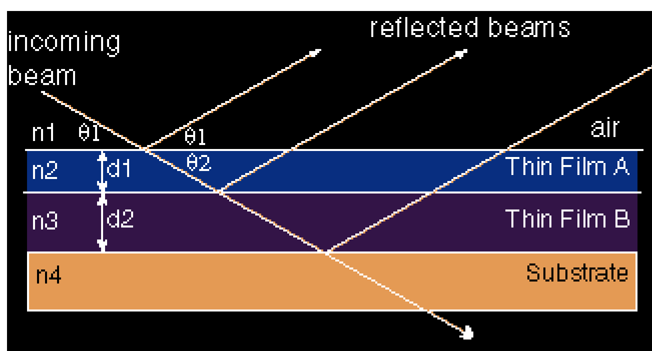

Figure 5. Reflectivity Geometry.

The x-ray reflectivity data shows oscillations (Kiessig Fringes) with wavelength, and these oscillations can be used to calculate layer thickness, density, roughness and other properties after fitting the data. As shown in Fig. 6, the spacing between the maxima of these oscillations correspond to the film thickness, and the value of the critical angle related to the film density. The roughness of interface or surface mainly determines the signal of the background.

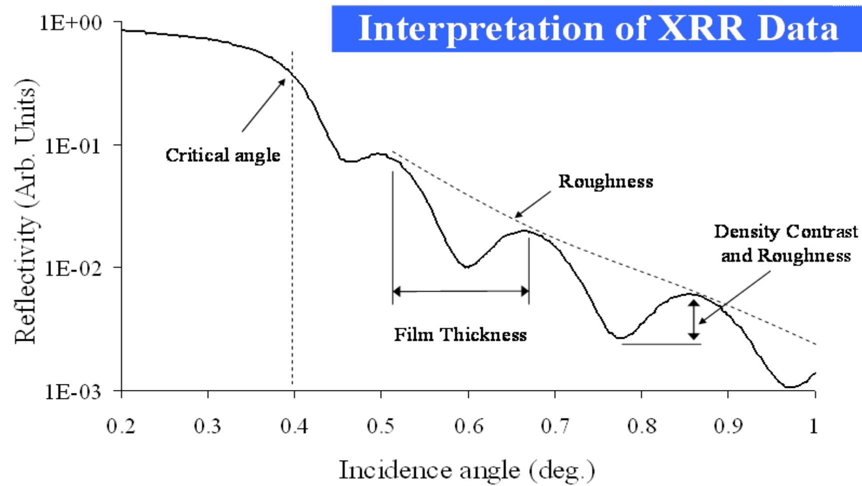

Figure 6. Interpretation of x-ray data

1.1.7 Atomic Force Microscopy

Atomic Force Microscopy (AFM) can provide a 3D profile of the surface on a nanoscale scale, by measuring the force between a sharp probe (<10 nm) and surface at a very short distance around 0.2 nm to 10 nm. The probe is supported on a flexible cantilever, which can touch the surface gently and record the small force between the probe and the surface at the same time.

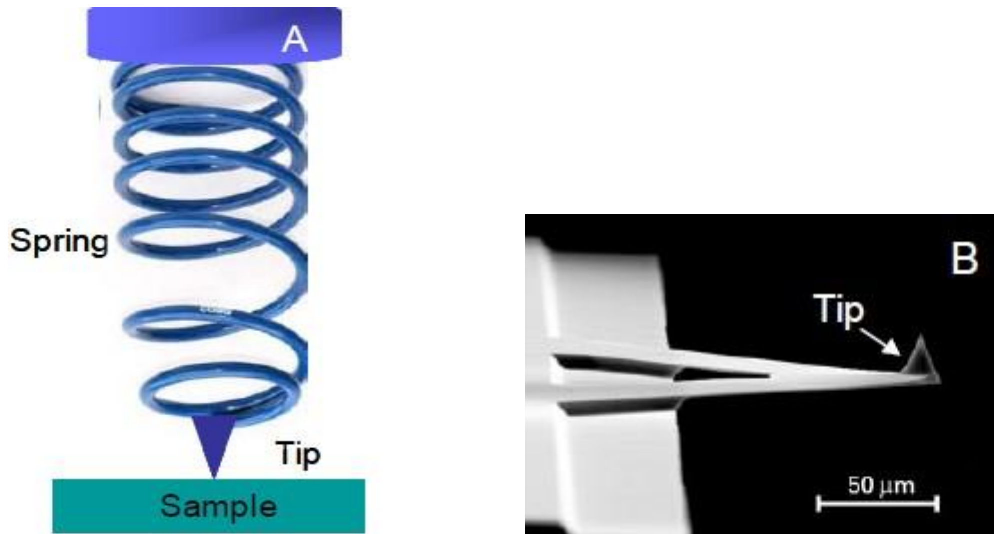

Figure 7. a) Spring depiction of cantilever.
b) SEM image of triangular SPM cantilever with probe (tip).

The probe is placed at the end of the cantilever, which can be considered it as a “spring”. The amount of the force between the probe and sample depends on the space between the probe and the sample surface, and the spring constant of the cantilever. The force can be calculated by Hooke’s Law:

$F=-kx$

Where F, k, and x are force, spring constant, and cantilever deflection, respectively.

Chapter 2 Review of the Literature

2.1 Glass transition temperature (T_g) behavior of polymer thin film study

Because T_g is directly related to the thermal stability of polymer thin films, the T_g of polymer thin films have been intensively studied by various methods, including ellipsometry [9-10], scanning probe microscope (SPM) [11-13], optical birefringence measurements [14], x-ray reflectivity [15-16], and dielectric relaxation [17-19]. After a series studies on the thickness dependence of T_g on supported polystyrene (PS) thin films prepared on Si substrates [9], it was broadly recognized that the reduction of T_g was observed with decreasing the film thickness and the reduction was considered in terms of a mobile surface layer [11,13]. Miyazaki [4] found that the T_g decrease with decreasing thickness of PS thin films below around 40 nm and the reduction becomes more significant when molecular weight becomes larger. For the thickness below around 10 nm, they also found T_g is independent of thickness around T_g= 354K. On the other hand, T_g increment with decreasing the thickness was found in poly (methyl methacrylate) (PMMA) thin films prepared on Si substrates with native oxide [9], which has a strong interaction. No matter whether T_g increasing or decreasing with thickness, the results implied the heterogeneous dynamics of polymer thin films along with the depth direction.

The unusual films thickness dependence of T_g has been considered in terms of quasimultilayer structures including a surface mobile layer, middle bulk-like layer, and bottom dead layer near the substrate. This quasimultilayer structure has been studied by fluorescence spectroscopy [20] and neutron reflectivity [21]. Inoue *et al.* [22] evaluated the distributions of T_g in multilayered thin films consisting of alternatively stacked deuterated PS and h-PS layers by using neutron reflectivity. They suggested that T_g of the total film thickness is mainly dominated by the T_g of the bottom layer. The most interesting thing is that only the bottom layer showed a quite small thermal expansivity and high T_g, which is too high to recognize within the experimental temperature range. It was broadly recognized that the anomalous physical property of the bottom layer could be related to the interaction between the polymer and substrate. Many researches have evaluated the T_g of the polymer thin film near the interface between polymer and substrate

from both direct [20, 23] and indirect methods [19, 24, 25]. The direct measurement of the T_g near the interface has been so far achieved only by the group of Tanaka [20] and the group of Ellison [23]. However, neither of them has observed a clear change of the bottom dead layer T_g compare to the bulk T_g. Until now, the final agreement of T_g near the interface between polymer and substrate of polymer thin film is still lacking.

2.2 Thermal expansion behavior (α) of polymer thin film study

Another interesting finding is the reduction of thermal expansivity a with decreasing the film thickness. In Kanaya's paper [4], their studies have investigated the thickness of PS thin films as a function of temperature by using x-ray reflectivity. The samples were annealed at 150℃ for 38 hours to avoid the structure relaxation during the measurements. They found that the thermal expansivity in the glass state decreases below the $2R_g$. In the melt state, the expansivity also keeps decreasing with decreasing thickness but the reduction is smaller than that in the glass state. While this phenomenon might be due to the dead layer near the substrate, the molecular mobility in PS thin films decreased with decreasing the film thickness, which might be a possible reason for the depression of a with the film thickness. This result also prove that the heterogeneity of polymer thin films along with the depth direction.

Inoue [22] used neutron reflectivity to study the distributions of T_g and thermal expansivity in PS multilayered films. One of the advantages using multilayered films in conjunction with neutron reflectivity is being able to evaluate the thermal expansivity of each layer directly. They found that the thermal expansivity of the bottom layer is almost zero, while those of the other layers are somewhat larger than the bulk value, independent of the location in the films. We expect the bottom layer is a “dead layer”, which with null expansion coefficients and the lack of molecular mobility.

2.3 Roughness behavior of polymer thin film study

Inoue *et al.* [22] evaluated the distributions of roughness in multilayered thin films. They found that the roughness was the largest at the topmost surface and the smallest near the bottom dead layer.

Kawaguchi *et al*. [26] also observed a similar enhancement of roughness at the topmost surface region compared to that with the bulk of polymer thin film.

2.4 Annealing effects on thickness of polystyrene thin film

Annealing is a heat treatment in which a material such as polystyrene is exposed to an elevated temperature for extended time and then slowly cooled. The effects of annealing are necessary to understand. For amorphous polymer such as polystyrene which usually exist in a non-equilibrium state at room temperature, thermal treatment can play an important role in changing the morphology. When the temperature is lower than T_g, the polymer chain are mainly immobile. However, when the temperature above T_g, the polymer will relax towards equilibrium in a process referred to as physical aging. It has found that the physical properties of films can be changed, because the morphology can be modified by annealing at the temperature higher than T_g [27]. The enthalpy and specific volume will decrease due to physical aging of a glass polymer with time at a rate dependent on temperature.

Kanaya *et al.* found that in the case of deuterated polystyrene thin films with the thickness of approximately 9 nm supported on silicon substrates, strongly annealing (135℃ for 12h) can cause positive thermal expansivity, while weakly annealing (80℃ for 12h) can cause negative thermal expansivity [15]. The former and latter annealing temperatures are 23℃ below and 32℃ above compared with T_g, respectively.

2.5 Substrate effect on polymer thin film

A substrate also shows an important role in deciding the polymer thin film behavior. Some thin film measurements point out that minor differences in material tension between a polymer and substrate, such as silicon oxide vs hydrogen passivated silicon, cause dramatically different film properties, especially inducing either positive or negative shifts in T_g [28, 29]. Hu and Granick [30] showed that the effect of the substrate on the poly(phenylmethylsioxane) viscoelastic properties extends to five or six times the radius of gyration away from a solid wall. Keddie [31] found T_g decreased for PS films on hydrogen-terminated silicon native-oxide substrate after heating up to 150℃ in air. Wallace and co-workers [32] showed an actual increase in root mean square (rms) roughness of the polymer/silicon interface from 5 to 11Å by using x-ray reflectivity, when the sample was exposed in air at 150℃ for 15 minutes. They [32] concluded that this kind of character at the interface might cause by the oxidation of the silicon surface, which illustrates the important of the character of the substrate is on determining the polymer thin film behavior.

Chapter 3 Materials and Methods

3.1 Solution Preparation

The samples used are polystyrene (PS) with molecular weight of M_w= 2.9×10^5 and molecular weight distribution (M_w/M_n=1.06) and PS with molecular weight of M_w= 5.0×10^3 and (M_w/M_n=1.06), where M_w and M_n are weight average and the number average of molecular weight, respectively. PS was dissolved in toluene.

Since film thickness can be controlled by the polymer concentrations, we prepared 0.09wt%, 0.2wt%, 0.17wt%, 1.2wt% and 2.5wt% of PS with M_w=2.9×10^5. For the concentrations by the weight of 0.09wt%, 0.17wt%, 1.2wt% and 2.5wt%, the thicknesses are around 4 nm, 7 nm, 50 nm and 120 nm respectively. Thickness was controlled varying by molecular weight; we also prepared PS (5.0×10^3) thin films from a solution 2.5wt%, resulting in 85 nm in thickness.

3.2 Substrate Preparation

The silicon wafer as the substrate was cleaved into 2cm*2cm squares. We washed the wafers by the following method to eliminate organic contaminants at the surface of the silicon wafers.

1. Wash the silicon by deionization water for several times.
2. Place the silicon wafers with the solution of H_2O:H_2O_2:NH_4OH under the ratio of 1:1:1, on the hot plate at 150°C to boil lightly for 20minutes to get the hydrophilic surface on the silicon wafers.
3. Wash the silicon wafer by deionization water for several times.
4. Clean the silicon wafers with the solution of H_2O:H_2O_2:H_2SO_4 blends of 1:1:1 composition by keeping it boil at 150°C for 20minutes.
5. Wash the silicon wafer by deionization water for several times.

6. Using the 1:10 ratio of Hydrofluoric acid (HF): H_2O blends around 15 seconds to remove the oxide surface on the silicon wafers to form the passivated silicon monohydride surface.

Our previous work has established that there is an oxide layer at 10-20Å in thickness on the Si surfaces prepared by this process, regardless of its crystal orientation.

3.3 Spin-cast films

PS thin films were prepared by spin-coating of toluene solutions on flat substrates. We used a photo-resist spinner (Headway Research Inc, 1-PM107D-R485) to spin at 2500 rpm for 30s.

3.4 Sample Annealing

It is expected that spin-cast films are stressed by strain during the spin-coating process, resulting in unrelaxed structures. Thus, the annealing temperature is very important for PS; it not only can remove the toluene from polymer films, but also relax the polymer structure. Kanaya *et al.* [26] reported that strongly or weakly annealed might cause different thermal expansivity for PS. For my thesis, except for the samples used for the first experiment which studied the effect of annealing condition, we fixed the annealing condition to 150℃ for 24 hours. The temperature (150°C) is higher than the bulk glass transition temperature (T_g = 100°C).

3.5 Washing by Toluene

In order to get the adsorbed layer, PS samples are immersed in a toluene solution for around half an hour, and then rinsed by toluene for five or six times. Checking the thickness by ellipsometry until the thickness does not change any more. The adsorbed layer shows null expansion coefficients.

3.6 Ellipsometry

After annealing the samples, we used ellipsometry to measure the thickness before further experiments. Ellipsometry measurements were performed with the Rudolph Research Ellipsometer, which can measure films thickness with angstrom resolution. Indexes of refraction (n) are variable, depending on a polymer. We used the n value of 1.575 for PS and determined the thickness.

3.7 X-ray Reflectivity

X-ray reflectivity experiments for PS thin films were conducted at the X10A beamline of the National Synchrotron Light Source (NSLS) at Brookhaven National Laboratory (BNL). The photon energy was 11.3KeV, i.e., x-ray wavelength of 1.09Å. The PS thin film samples were set in the high temperature vacuum chamber customly made with two kapton windows and investigated the T-dependence of the thickness from 25°C to 150°C for every 10°C or 20°C step.

3.8 Atomic Force Microscopy

The atomic fore microscopy (AFM) is a powerful technique used for investigating a wide range properties on the nanometer scale. It has always been used to characterize the morphology of the thin polymer film by analyzing the topography, friction and phase separation under the tapping mode. Using the AFM, I could get the morphological images of the surfaces.

Chapter 4 Experiment Results and Discussion

1st Experiment --- Thickness of adsorbed layers depends on the annealing time.

This experiment is to study the relationship between the thickness of adsorbed layers and annealing time. There are two groups of samples. The first group was prepared a concentration of 2.5wt% and the second group was prepared from a PS concentration of 0.2wt%. I prepared four samples for each group with different annealing times, with 1, 2, 4 and 6 h.

1. Samples were spin cast from toluene onto clean hydrogen-passivated Si wafers.
2. Samples were kept in a vacuum oven at 150°C with different annealing times of 0, 1, 2, 4, and 6 hours.
3. Washing the samples by toluene to obtain the adsorbed layer.
4. Measured the thickness by ellipsometry.

(i) PS (M_w=290K, C=2.5wt %)

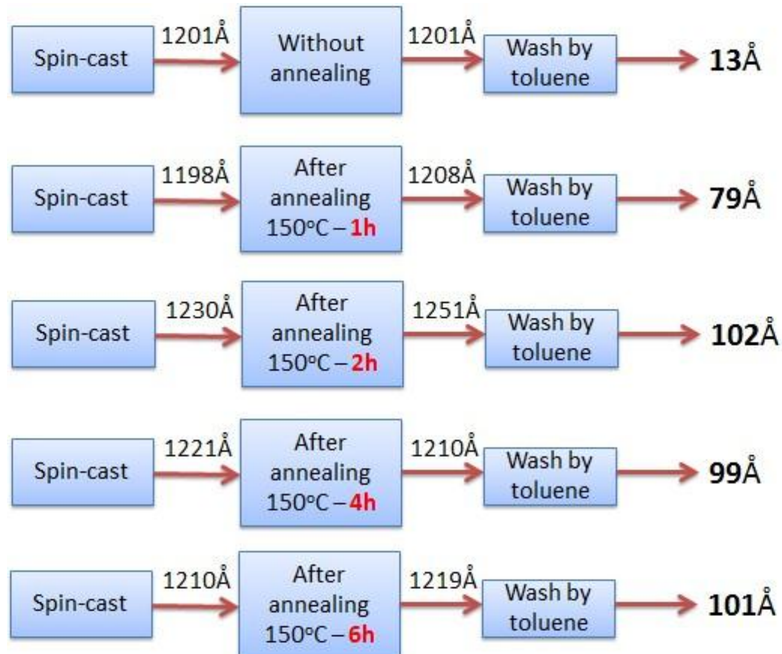

Figure 8. Process and data for the experiment of PS (M_w=290K, C=2.5wt%).

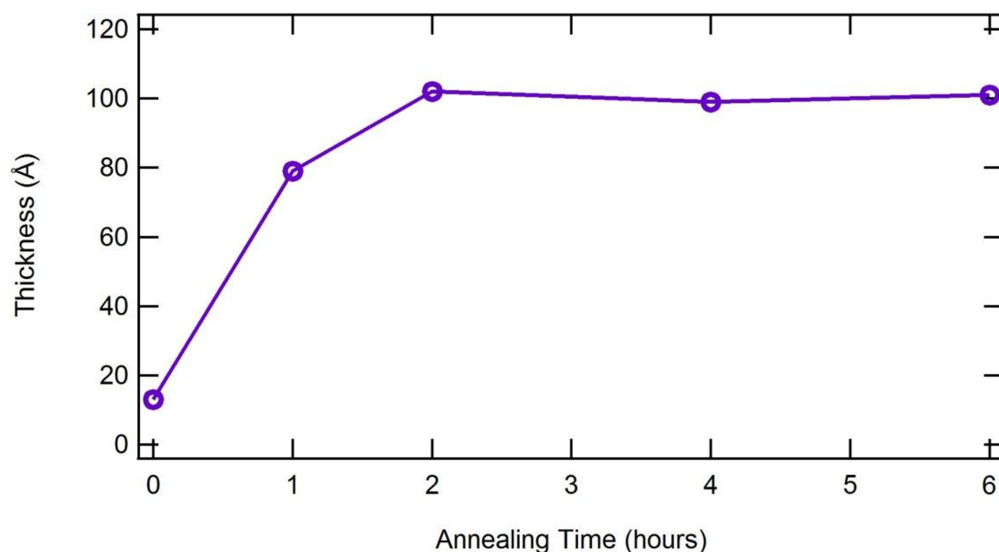

Figure 9. Thickness of adsorbed layer from ellipsometry vs annealing hours

Figure 9 shows the thickness change as a function of annealing time. From the figure, we can see there is a significant increase from 13Å to 100Å in the first two hours annealing, and then thickness remains constant after 2 hour annealing time.

We also used x-ray reflectivity to determine the thickness at room temperature. The data was fitted by a three layer model, i.e., Si layer, SiO_2 layer, and polymer layer.

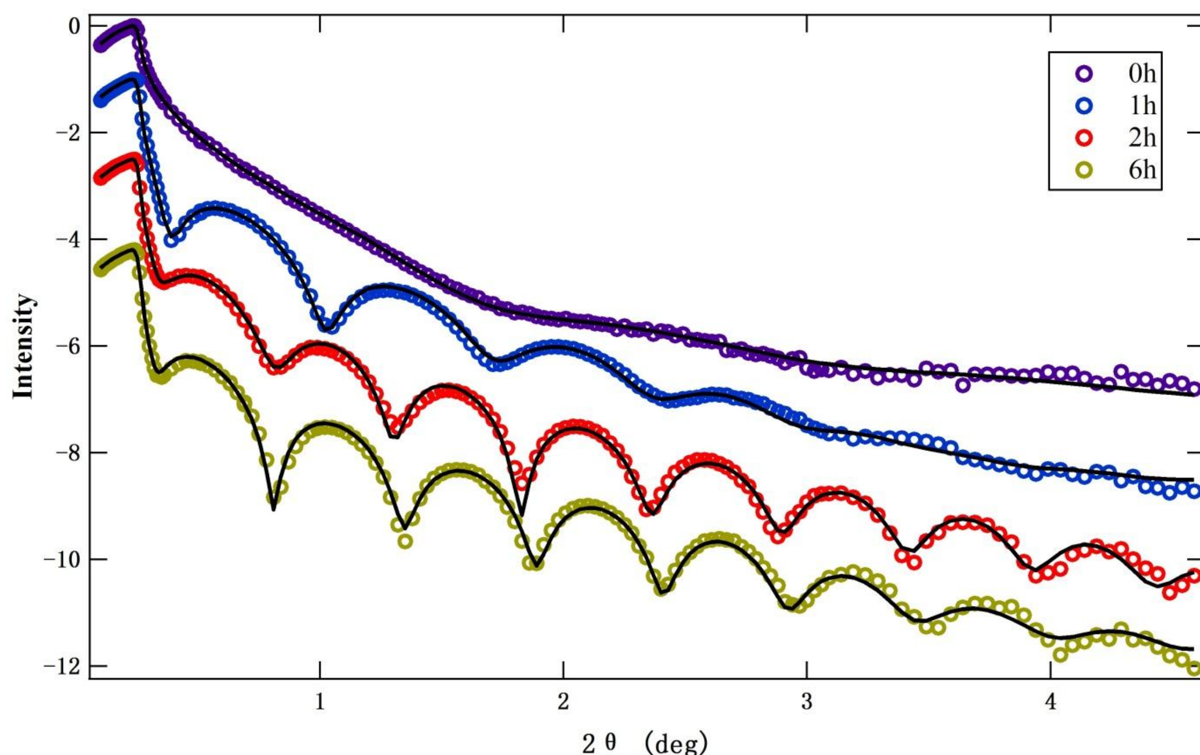

Figure 10. Specular reflectivity profiles and their corresponding modeled fits (solid lines) measured for polystyrene films (290K 2.5wt%) with varying annealing time.

Annealing Time (hour)	Thickness (Å)	delta δ ($\times 10^{-6}$)
0	**5.8**	**0.45**
1	**73.3**	**1.11**
2	**95.4**	**1.11**
6	**93.5**	**1.12**

Table 1. Calculated thickness and delta for PS (M_w=290K, 2.5wt%) with different annealing time.

From the best fitting results, we can see that the thickness of the adsorbed layer increased from 5.8Å for annealing time 0h to 95Å for 2h, then keep stable after 2h annealing. The same behavior also can be seen from delta, from 0.45×10^{-6} to 1.11×10^{-6}. The number becomes closer to the delta of bulk layer (1.1×10^{-6}).

The graphs of delta vs annealing time and thickness vs annealing time are as follow, which can better show the behavior of delta and thickness with annealing hours clearly.

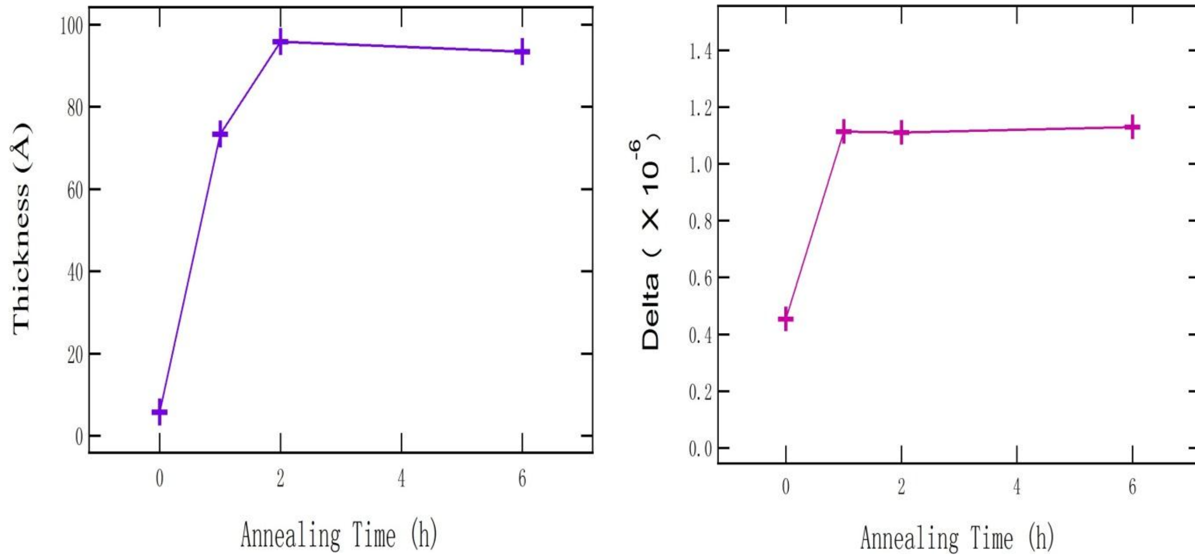

Figure 11. Thickness and delta of adsorbed layer PS (M_w=290K, C=2.5wt%) vs annealing time.

(ii) PS (M_w=290K, C=0.2wt%)

By using a different concentration of a PS solution, we aim to clarity the effect of the concentration on the adsorption process of polymer chains.

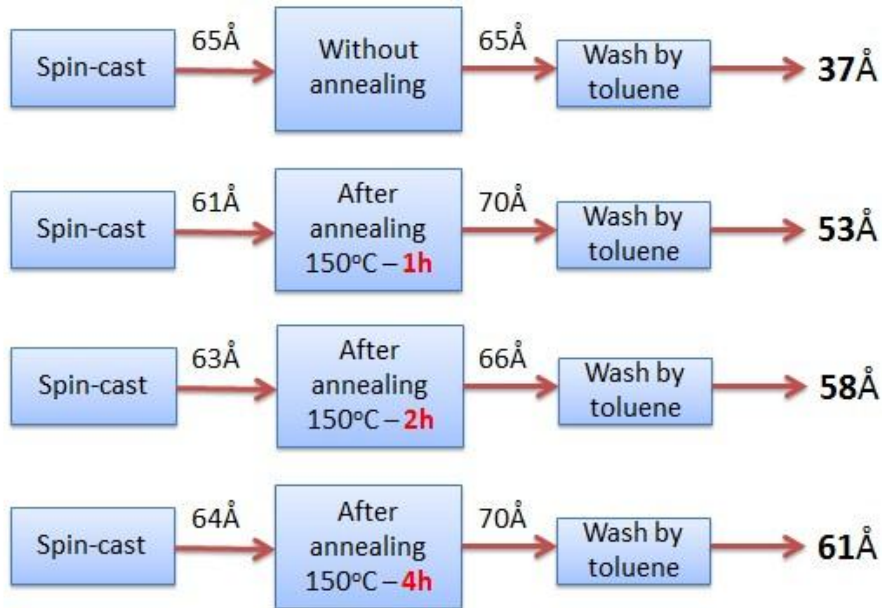

Figure 12. Process and data for the experiment of PS (M_w=290K, C=0.2wt%).

We also characterized the films by using x-ray reflectivity at room temperature in air. Representative x-ray reflectivity are shown in Figure 13.

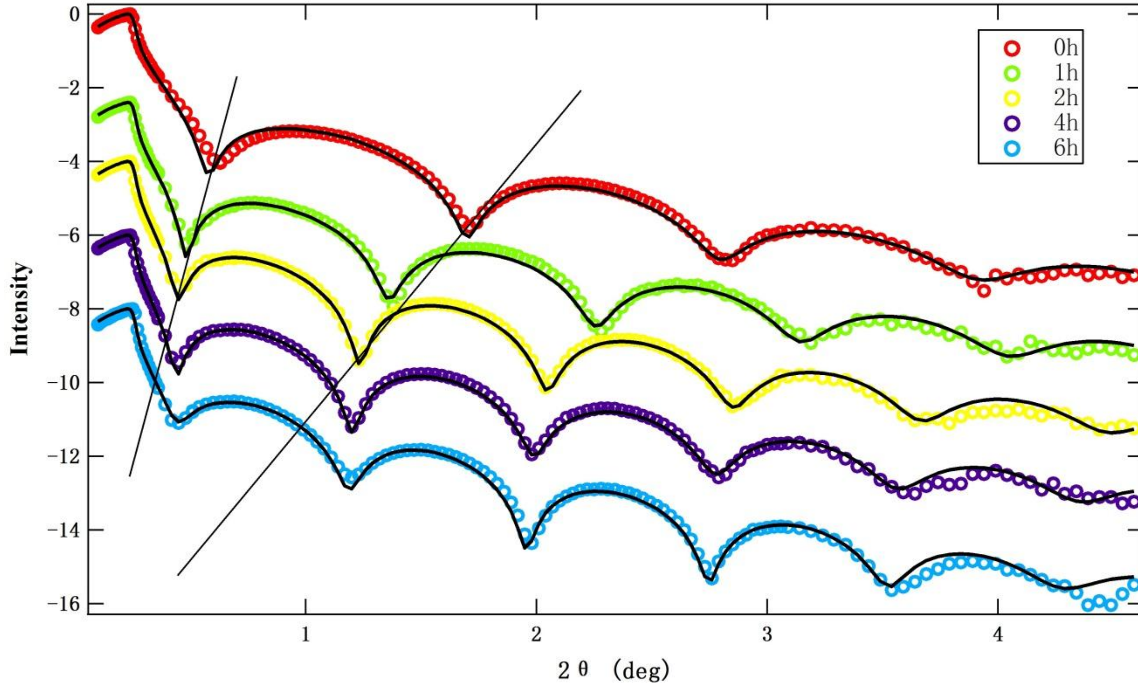

Figure 13. Specular reflectivity profiles and their corresponding modeled fits (solid lines) measured for polystyrene film (M_w=290K, C=0.2wt%) with varying temperature.

The results of the fits using a three layer model are shown in Table 2.

Annealing time (hour)	Thickness (Å)	Delta ($\times10^{-6}$)	Roughness (Å)
0	44.3	1.14	4.5
1	55.5	1.23	2.5
2	61.2	1.20	3.2
4	62.9	1.23	3.1

Table 2. Calculated thickness and delta for PS (M_w=290K, C=0.2wt%) with different annealing time.

Figure 14 shows the delta vs annealing time and thickness vs annealing time.

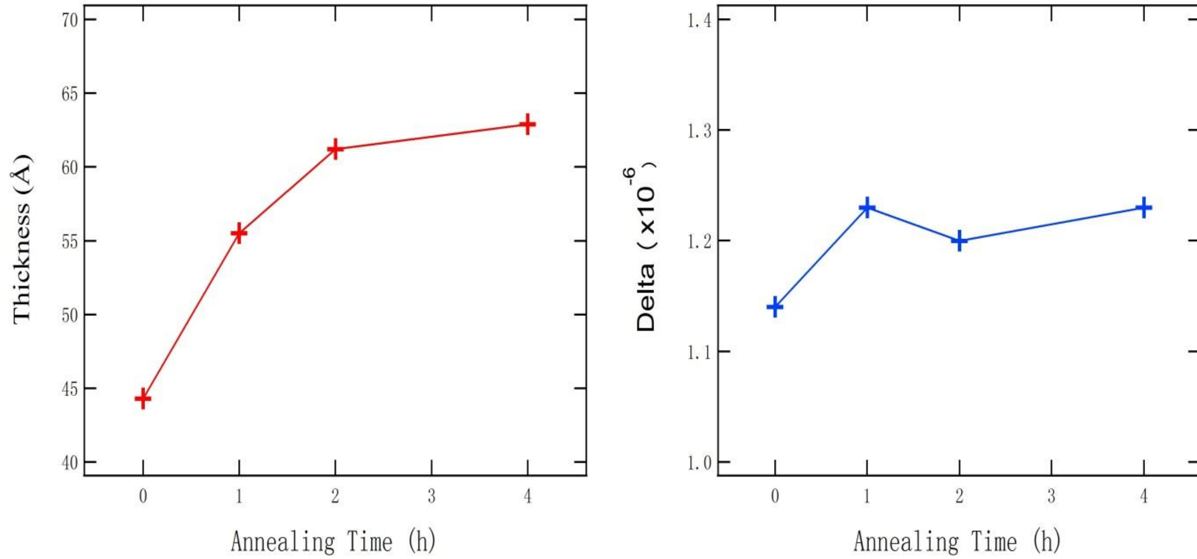

Figure 14. Thickness and delta of adsorbed layer PS (M_w=290K, C=0.2wt%) vs annealing time.

From the fitting results, we can see that the thickness of the adsorbed layer increased from 44Å for 0h to 63Å for 2h annealing. After 2 hours annealing, the thickness remains almost constant.

The delta of the adsorbed layer has increased from 1.14×10^{-6} to around 1.20×10^{-6} in the first hour annealing, and then keep stable around 1.20×10^{-6}, which is closer to the delta of final dead (1.20×10^{-6}). The result shows the final dead layer structures are always high density ($\delta=1.2\times10^{-6}$). The thickness increases with increasing concentration.

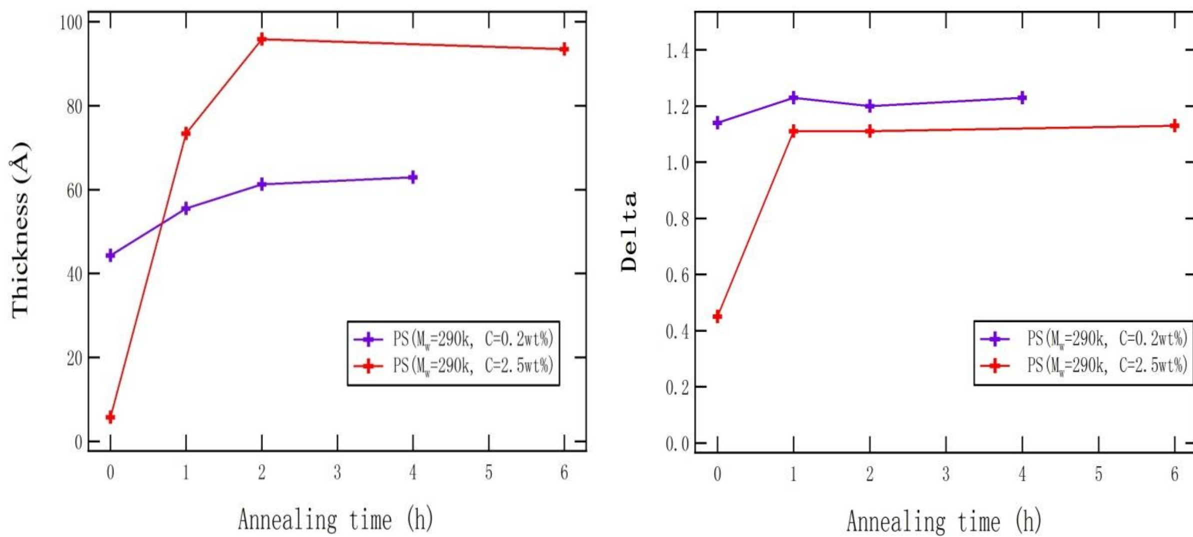

Figure 15: Delta and thickness vs annealing time by different concentration.

Compared with the first and second experiment, the thickness of the adsorbed layer for both cases increases in the first 2 hours annealing, and then becomes nearly constant after 2h. Similar trend can be seen in δ. From here we may conclude that the higher concentration polymer solution can provide a much thicker layer, but for 0.2wt % can give a similar conformation of the adsorbed layer.

2nd Experiment --- Dead layer

Our objective is to study how long does it take to get the final dead layer by immersing the PS spin-cast film in toluene.

Gin and co-worker showed that the final dead layer for PS (M_w=290K) is around 40Å after super-critical carbon dioxide process. However, my data shows that the adsorbed layer for PS (M_w=290K) is about 90Å after the leaching process with toluene for 20min. Thus, I anticipate that the leaching time for my samples is not enough.

I put one adsorbed PS layer in toluene for a long time, and check the thickness change as time goes. The sample was PS (M_w=290K, C=2.5wt %) with initial thickness around 1500Å, which had been annealed at 150°C (50°C above the T_g =100°C) for 24h before washing by toluene. The process is as follow:

Figure 16. Process and data of the second experiment.

I measured the thickness change in the last 140 days for about five months by using ellipsometry. Figure 17 shows the time dependence of the residual layer.

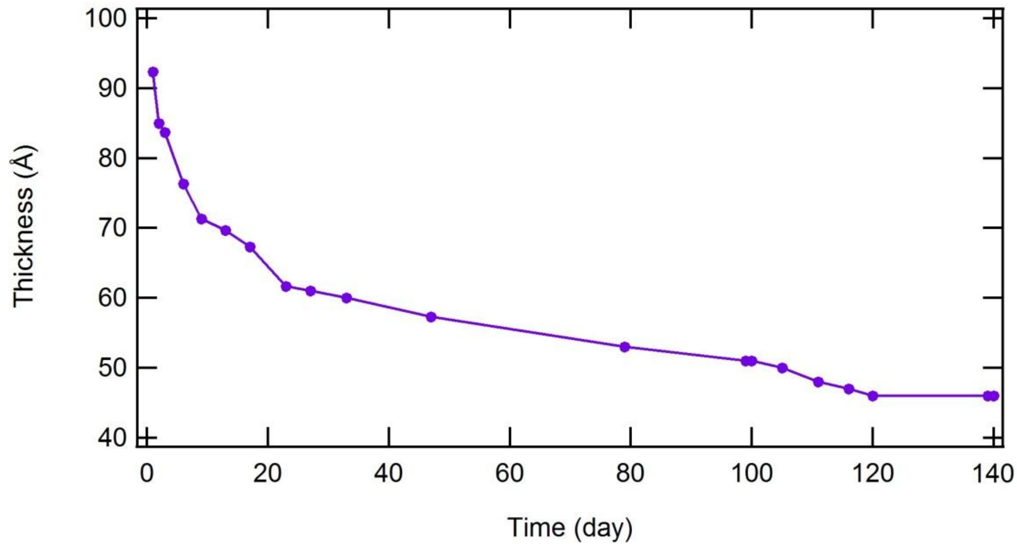

Figure 17. Thickness of adsorbed layer vs days immerse in toluene in air condition.

From the figure, we can see that the thickness of the adsorbed layer decreased with increasing time, from 92Å to 46Å after 120 days immersed in toluene at room temperature. Compared with Gin's about the thickness of the final dead layer (40Å), which was obtained by using super-critical carbon dioxide condition, the result proves that it takes almost 120 days to achieve the final thickness of the adsorbed layer by using toluene alone.

3rd Experiment --- Study the molecular mobility of PS adsorbed layers

The objective of this experiment is to prepare another PS adsorbed layer on top of a adsorbed layer.

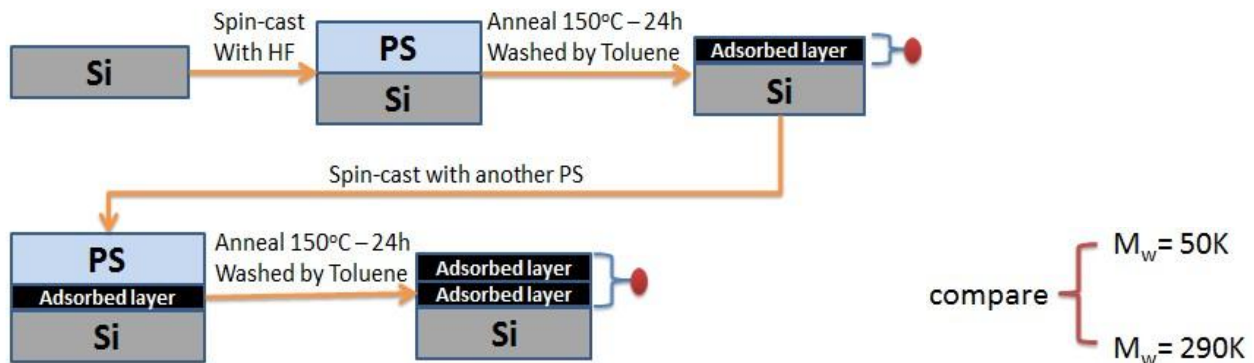

Figure 18. Procedure used for the third experiment.

1. Two PS (M_w=290K, C=2.5wt %) and PS (M_w=50K, C=2.5wt %) were spin cast from toluene solutions onto clean Si wafers pretreated with a hydrofluoric acid solution. The thicknesses were around 1400Å and 870Å, respectively.

2. Annealing the samples at 150°C ($T>T_g$ =100°C) for 24h.

3. Washing the samples by toluene to obtain the adsorbed layer.

4. Checking the thickness by ellipsometry. The thickness of the adsorbed layers for PS (M_w=50K) and (M_w=290K) were 46Å and 100Å, respectively.

5. The samples then were spin cast again onto the first adsorbed layer.

6. Annealing the sample at 150°C ($T>T_g$ =100°C) for 24h.

7. Washing the sample by toluene to obtain the adsorbed layer.

8. Finally, measured the total thickness by ellipsometry. The results were 52Å and 94Å for PS 50K and 290K, respectively. The processes are as follow:

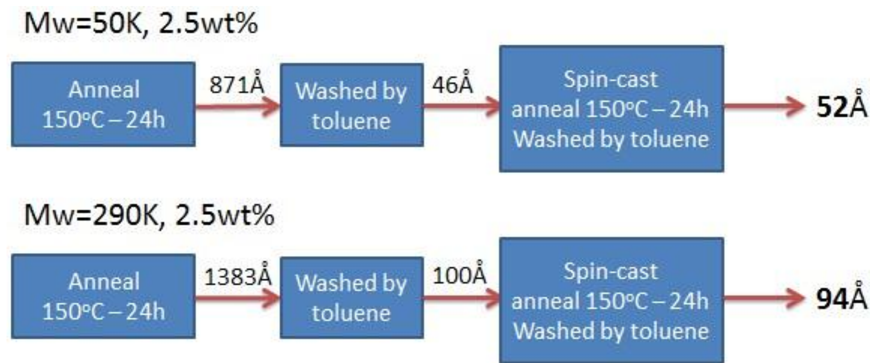

Figure 19. Procedure and data used for the third experiment.

Considering the possible errors in the measurement from ellipsometry, the total thickness doesn't change much after spinning cast another PS layer attached on the adsorbed layer substrate. This means the additional spin cast layer cannot prepare on top of the adsorbed layer. This behavior shows that the adsorbed layer almost absence of molecular mobility as well as attachments to solid substrate.

After the first adsorbed layer being created after 150°C for 24h annealing, the polymer chain have occupied the whole space of Si substrate, so that there is no enough space for the additional polymer to fully attach.

4th Experiment --- X-ray reflectivity results for PS 4nm, 9nm and 50nm

Here I prepared 4nm in thickness spin-cast PS (M_w= 290K) thin films to compare the structure with the PS dead layer whose thickness is nearly identical. Further, I also measured the T-dependence of the thickness by using high temperature x-ray reflectivity.

Figure 20 shows the x-ray reflectivity profiles for the spin-cast PS film (4nm in thickness, anneal 90℃ for 1h) as a function of temperature.

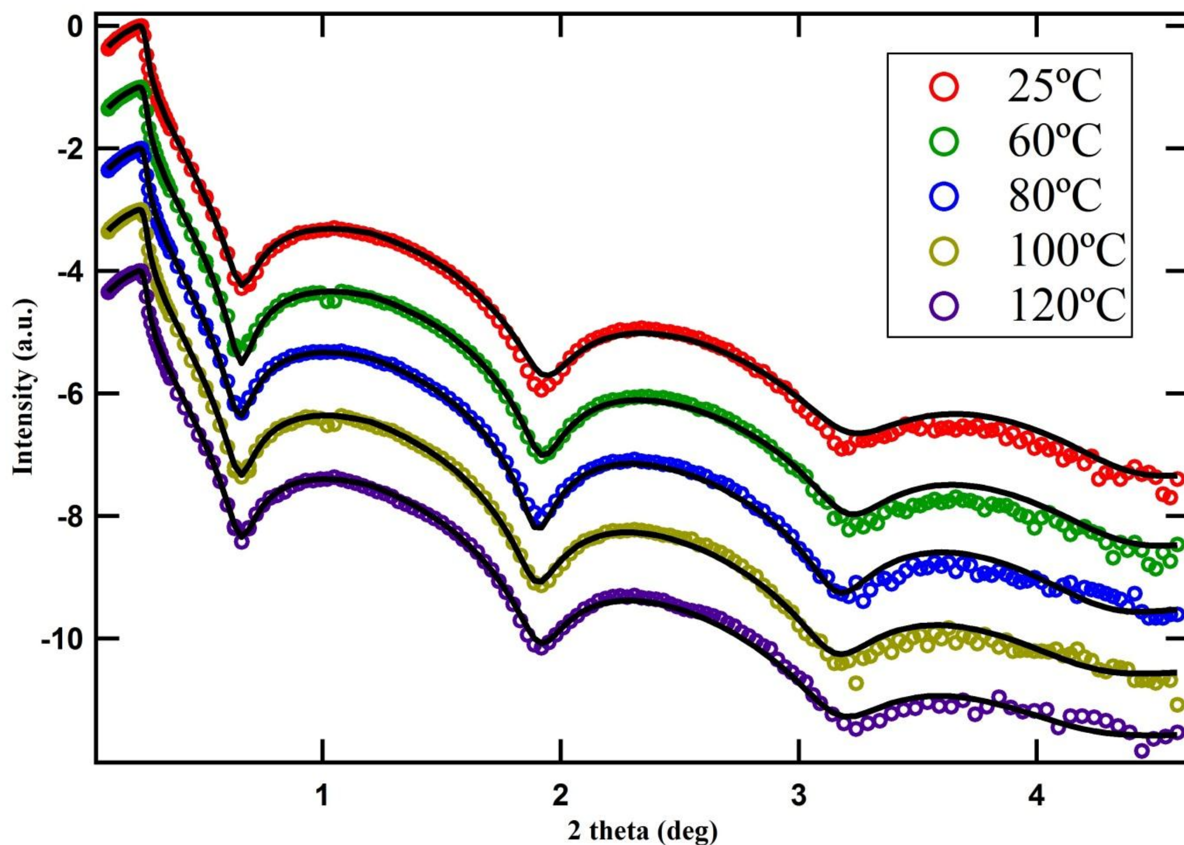

Figure 20. Specular reflectivity profiles and their corresponding modeled fits (solid lines) measured for PS (4nm in thickness, 90℃ for 1h annealed) in air with varying temperature.

The fitting results using a three layer model are shown by the soild lines. From the fitting results, we can see that the first fringe and second fringe does not shift with temperature increasing, indicating the thickness doesn't change much from 25℃ to 120℃. Table 3 summarizes the fitting results.

Temperature (℃)	Thickness (Å)	Delta (×10^{-6})	Roughness(Å)
25	38.9±0.4	1.33±0.02	3.5±0.1
25	38.3±0.4	1.28±0.02	3.7±0.1
Turn off heater and cool down in air			
60	39.1±0.4	1.32±0.02	4.1±0.1
80	39.6±0.4	1.33±0.02	4.2±0.1
100	39.4±0.4	1.11±0.02	5.6±0.1
120	39.4±0.4	1.10±0.02	5.9±0.1

Table 3. Thickness, delta and roughness for PS (4nm in thickness, 90℃ for 1h annealed) with increasing temperature in air.

Figure 21 shows the thickness and delta values of PS (M_w=290K, 4nm in thickness, 90℃-1h annealed) as a function of temperature.

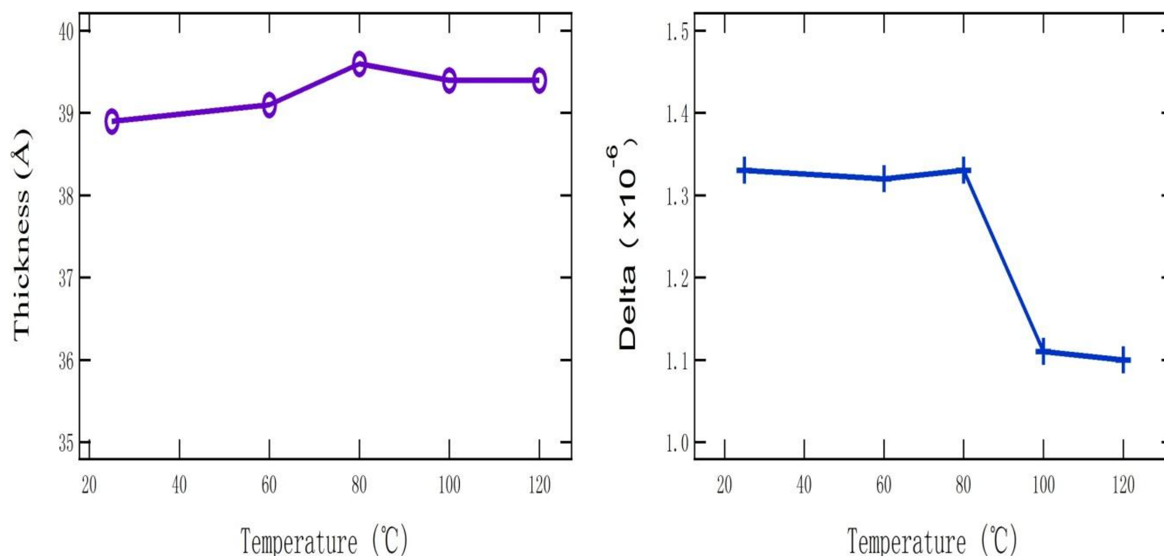

Figure 21. Thickness and delta for PS (4nm in thickness, 90℃ -1h annealed) vs temperature, measured in the air.

The delta values remain constant around 1.3×10^{-6} in first two hours annealing, and then decreased slightly to around 1.1×10^{-6} when the temperature reaching to 100℃, which correspond to the bulk T_g of PS.

This data may suggest that 1-hour annealing time at 90℃ is not enough to remove toluene. Thus, I prepared another sample (4nm in thickness) with 24h annealing at 150℃ to see my hypothesis.

Figure 22 shows the x-ray reflectivity results for PS film (4nm in thickness, anneal 150℃ for 24h) measure in air.

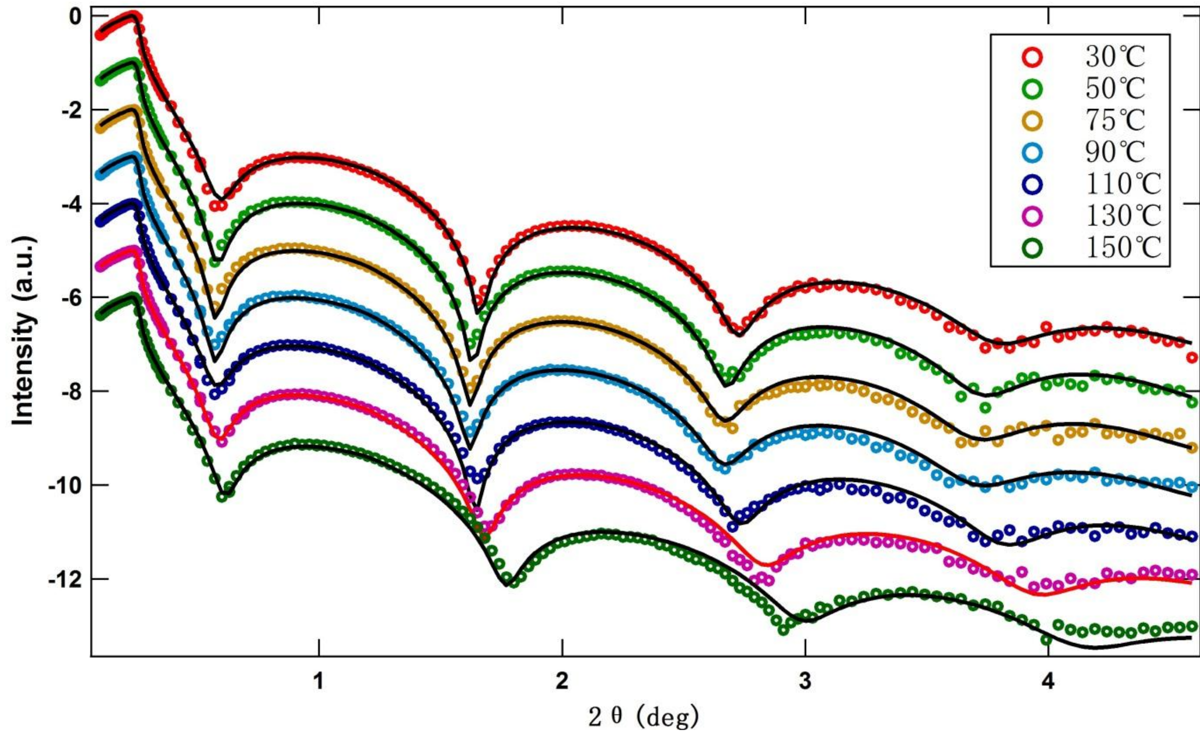

Figure 22. Specular reflectivity profiles and their corresponding modeled fits (solid lines) measured for PS (4nm in thickness, 150℃ for 24h annealed) in air with varying temperature.

The best fitting results using a three layer model are shown indicated by the solid lines. The fitting results are also shown in Table 4.

Temperature (℃)	thickness (Å)	Delta ($\times 10^{-6}$)	roughness(Å)
30	45.7	1.10	2.9
40	46.0	1.11	3.0
50	46.5	1.18	3.2
60	46.6	1.14	3.2
75	46.8	1.20	3.3
90	46.8	1.18	3.4
90 X-ray refill	46.4	1.16	3.4
100	46.1	1.17	3.5
110	45.7	1.09	3.5
120	45.0	1.12	3.6
130	44.3	1.10	3.6
140	43.5	1.09	3.7

150	42.0	1.08	3.6

Table 4. Thickness, delta and roughness for PS (4nm in thickness, 150℃ for 24h annealed) with increasing temperature in air.

Figure 23 shows the thickness and delta values of PS (M_w=290K, 4nm in thickness, 150℃-24h annealed) as a function of temperature.

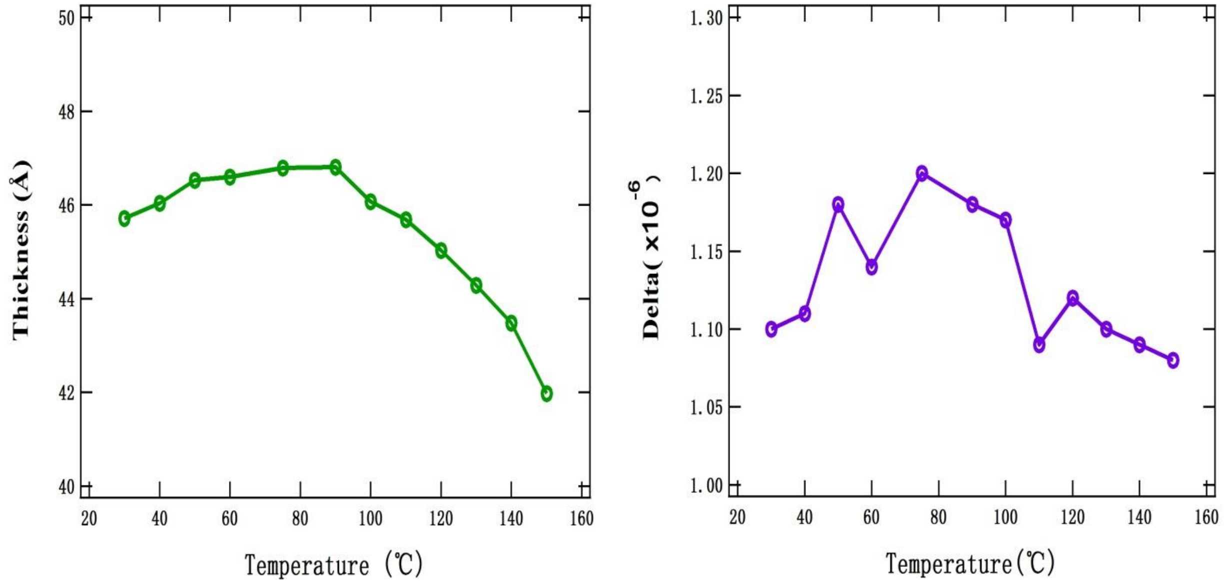

Figure 23. Thickness and delta of PS (4nm in thickness, 150℃ -24h annealed) vs temperature, measured in the air.

Using the following equation, we calculated thermal expansion coefficient α with different data of temperature dependence of the film thickness:

$$\alpha(T) = \frac{h\left(T + \frac{\Delta T}{2}\right) - h\left(T - \frac{\Delta T}{2}\right)}{h_0 \Delta T}$$

where *α(T)* is the temperature-dependent expansivity, *h(T)* is the temperature-dependent thickness, h_0 is a reference thickness, and ΔT is the differentiation range.

For PS, the thermal expansion coefficients are calculated as follow:

α (40℃-60℃) = $6.02\times10^{-4}K^{-1}$

α (60℃-90℃) = $2.24\times10^{-4}K^{-1}$

From the fitting results, we can see that the thickness increased gradually from 30°C to 90°C. At T > 90°C, the thickness started to decrease. However, the present results are different from Kanaya's data, which present the thickness decreased at T < 70°C.

It is apparent that the intermolecular interaction can result capillary forces which are capable to retract a purely liquid film from a solid surface [33]. Gunter found that the intermolecular interactions responsible for capillary forces may be sufficiently strong to deform even quasisolid films [34]. However, some theory expected [35] that elastic effects could even steady thin films and hinder them from dewetting. One possibility of film dewetting via surface diffusion [36] or evaporation/condensation [37-39] can be rule out due to the large number of chemically linked monomers and the practically zero vapor pressure of long chain polymers. It seems until now dewetting of long chain polymers at temperatures close to their glass transition is not yet fully understood.

Also we can see that the spin-cast PS (4nm in thickness) thin film have a lower delta ($\delta = \sim 1.10\times10^{-6}$), which is in good agreement with the bulk ($\delta = \sim 1.14\times10^{-6}$), compared with the adsorbed layer or real dead layer ($\delta = \sim 1.30\times10^{-6}$). This may suggest that the polymer chain conformation maybe different, even the thickness is about the same.

A polystyrene film around 4nm was further characterized by using only atomic force microscopy (AFM) at room temperature after high temperature x-ray reflectivity experiments.

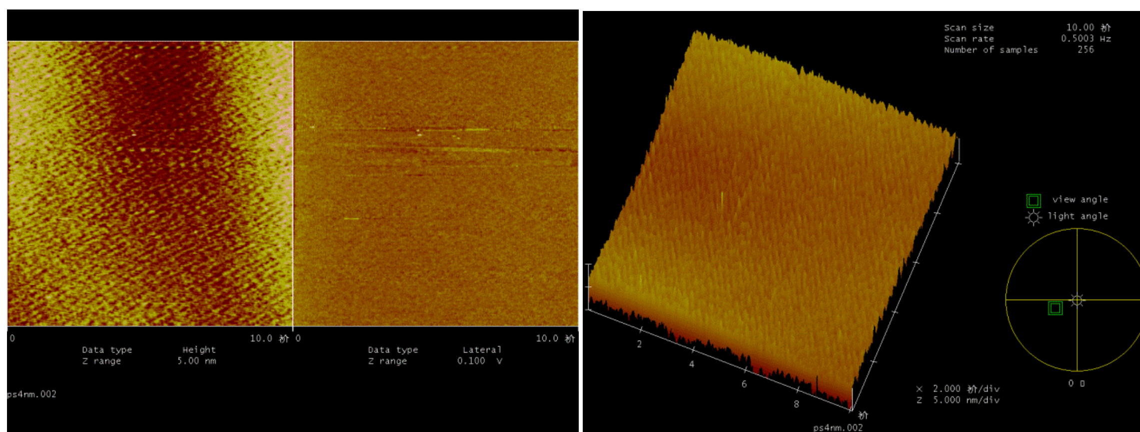

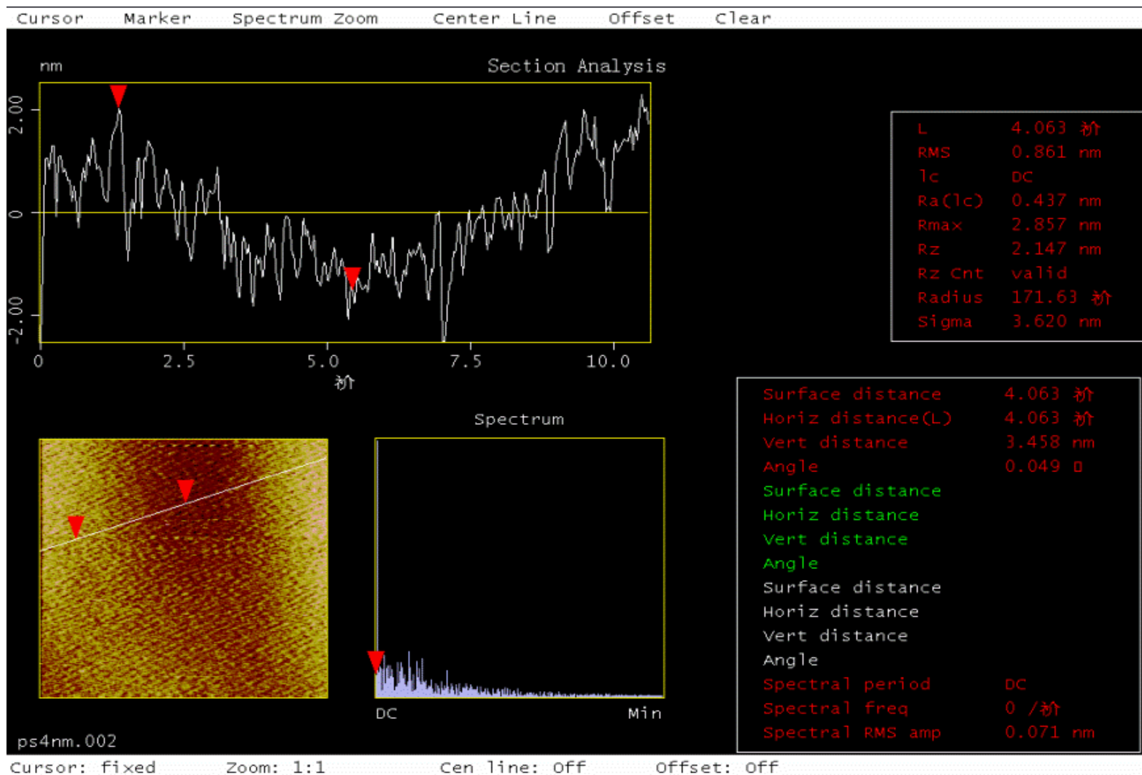

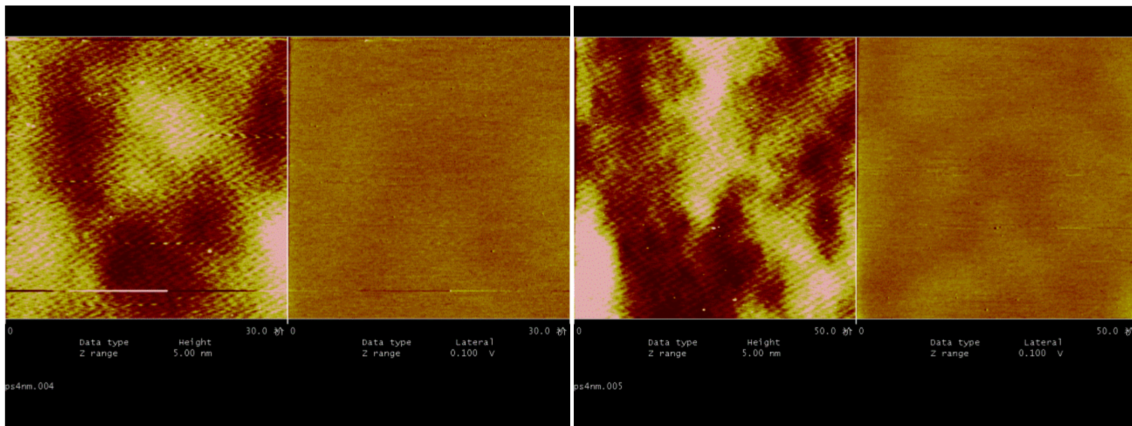

Figure 24: AFM image for PS (M_w= 290K, 4nm in thickness, 150℃ -24h annealed)

From the AFM images, we can see that there is no sign of de-wetting (no holes). The cross sectional image show that the RMS roughness is around 3nm, which is almost identical to that of the total film thickness.

Figure 25 shows the x-ray reflectivity profiles for the spin-cast PS film (M_w=290K, 4nm in thickness, anneal 150°C for 24h, measure the thickness in vacuum) as a function of temperature.

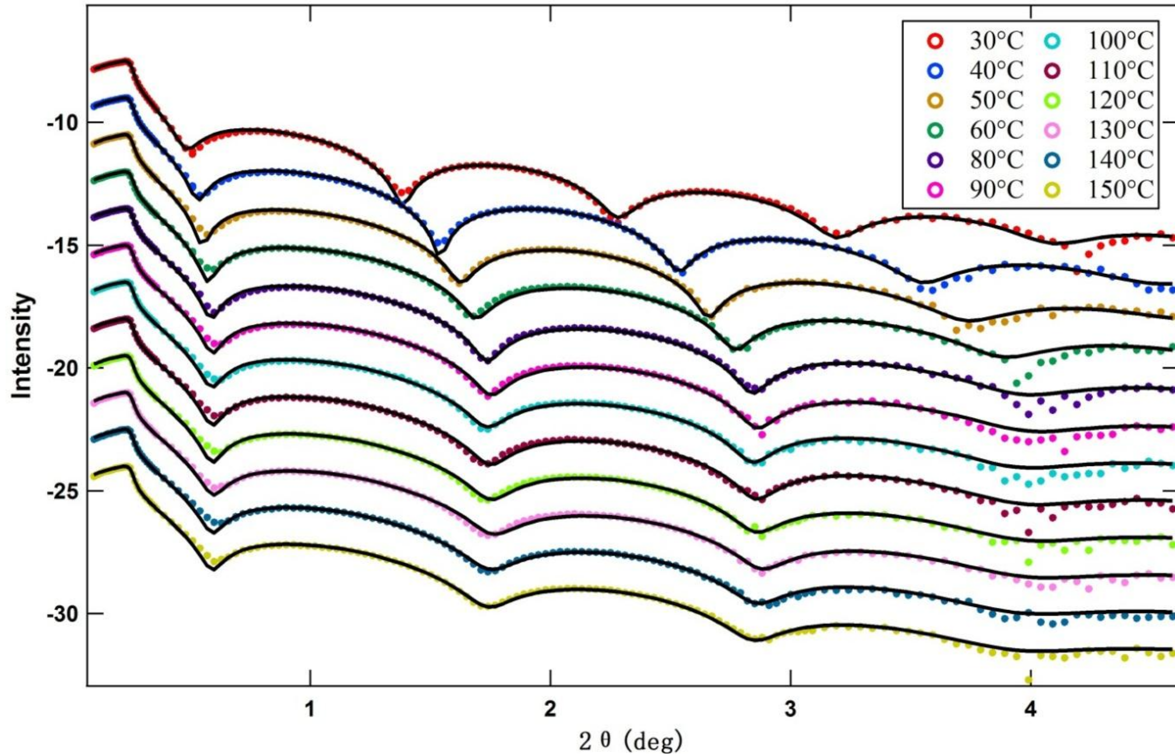

Figure 25. Specular reflectivity profiles and their corresponding modeled fits (solid lines) measured for PS (4nm in thickness, 150℃ for 24h annealed) under vacuum with varying temperature.

The fitting results are using a three layer model are shown by the solid lines. Table 5 summarizes the fittting results.

Temperature (℃)	Thickness (Å)	Delta (×10^{-6})	Roughness (Å)
25	54.5	1.13	4.9
30	54.8	1.11	4.6
40	49.2	1.16	4.7
50	46.8	1.28	4.8
60	44.9	1.29	4.4
80	43.8	1.30	5.0
90	43.4	1.31	5.0
100	43.8	1.33	5.0
110	43.5	1.32	5.0
120	43.5	1.32	4.9
130	43.2	1.34	5.0
140	43.5	1.33	4.9
150	43.7	1.34	5.1

Table 5. Thickness, delta and roughness for PS (4nm in thickness, 150℃ for 24h annealed) with increasing temperature under vacuum.

Figure 26 shows the thickness and delta values for PS (4nm in thickness, 150℃ for 24 h annealed, measures in vacuum) as a function of temperature.

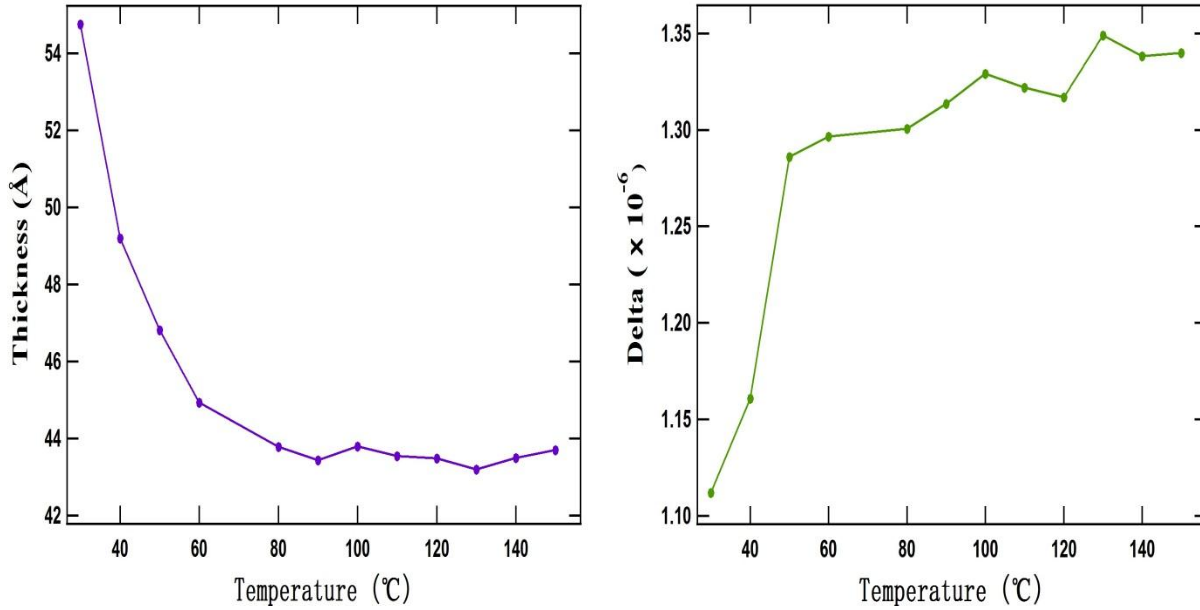

Figure 26. Thickness and delta of PS (M_w=290K, 4nm in thickness, 150℃-24h annealed) vs. temperature under vacuum.

From the observed and fitting profiles, we can see that the thickness decreased significantly within the T-range from 30℃ to 80℃. After 80℃, we observed zero or quite small thermal expansivity. The possibility might because the polymer begins to de-wet or even degrade after high temperature experiments under vacuum. Thus, I checked the thickness again at 30℃ after the heating experiments. The sample was kept in vacuum condition until the temperature decreased to 30℃.

Using the following equation, we calculated Thermal Expansivity efficiency α by different data of temperature dependence of film thickness.

$$\alpha(T) = \frac{h\left(T + \frac{\Delta T}{2}\right) - h\left(T - \frac{\Delta T}{2}\right)}{h_0 \Delta T}$$

α (30℃-50℃) = $-8.06\times10^{-3}K^{-1}$

α (40℃-60℃) = $-4.56\times10^{-3}K^{-1}$

α ($T>T_g$)= 0

Temperature (℃)	thickness (Å)	Delta (×10^{-6})	Roughness (Å)
Back to 30	58.5	0.99	4.9
Initial 30	54.8	1.11	4.9

Table 6. Data compared at 30℃ before and after experiment.

We found the thickness returned to the origin thickness around 58Å, indicating the phenomenon is not due to dewetting but the reversible behavior. After measuring XR, we measured the surface and confirmed that no dewetting occurs.

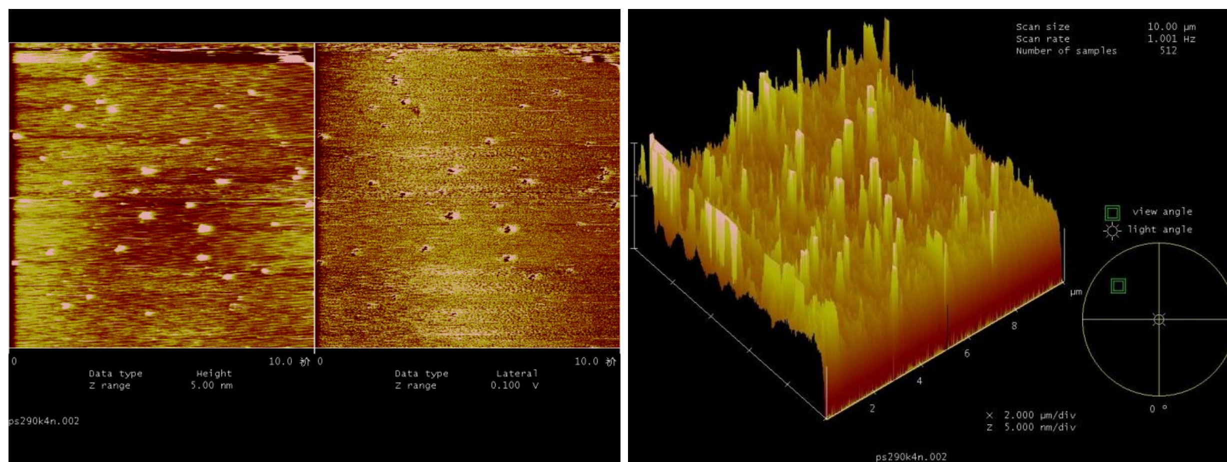

Figure 27: AFM image for PS (M_w=290K, 4nm in thickness, annealed 150℃ for 24h, measured under vacuum)

William and his group [16] found the negative expansivity for ultra PS thin films in Figure 34. The contraction occurred at temperature below the bulk T_g, the range from 0%-17% depending on the initial film thickness. On should note that the molecular weight M_c=573000, the radius of gyration R_G for polystyrene in the melt is 212Å and the persistence length is approximately 9Å. Their sample annealed at 90℃ for 1 hour and then allowed to cool down to 30℃. Their XR experiments were also performed under vacuum from room temperature to 80℃ in 10℃ increments. The film thickness contracted from 45.2Å to 39.3Å during this temperature cycle. After cooling the film back to 27℃, the thickness returned to 47.4Å.

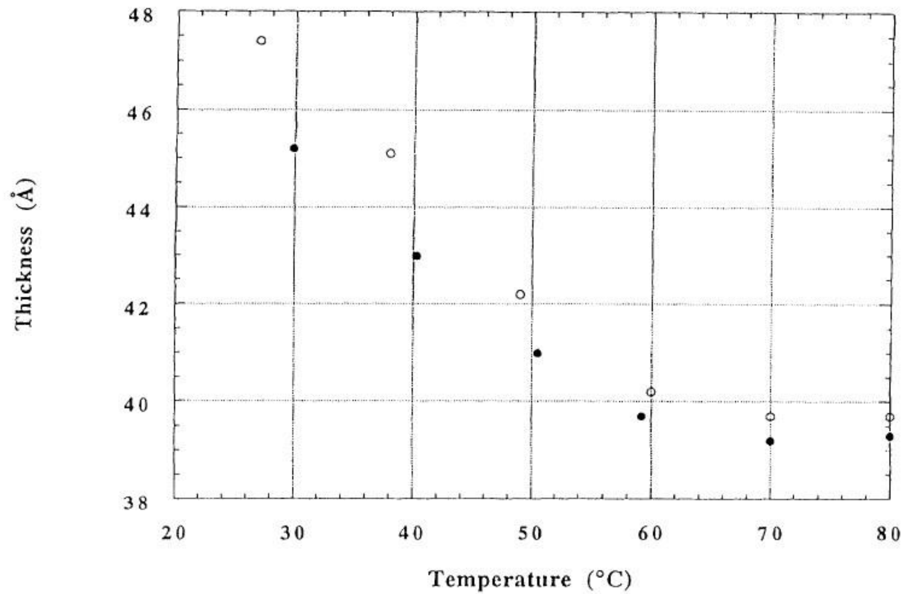

Figure 28. An ultrathin polystyrene film was annealed and then heated incrementally to 80℃, cooled, and then reheated to 80℃. The first heating cycle are showed as black dots, and the second heating cycle are showed as write dots. [16]

However, Kanaya proposed the negative thermal expansivity seen in William's experiments is caused by unrelaxed structures due to lack of sufficient annealing. [15] They studied the effects of the annealing the thickness of PS thin films by using neutron reflectivity and found that the annealed PS film at 80°C for 12h show negative expansivity in the glass state, while the PS films with the thickness more than 90Å (Figure 29) annealed at 135°C for 12h. One should note that the sample they used was deuterated (PS-d_8) with M_w= 300000. Before spin-coating, silicon wafers were rinsed by toluene, acetone, methanol and then distilled water. Native oxide layer remained on the surface was not removed from the wafer in their experiment. After annealing, the samples were kept at room temperature (25°C) for about one week before measurements.

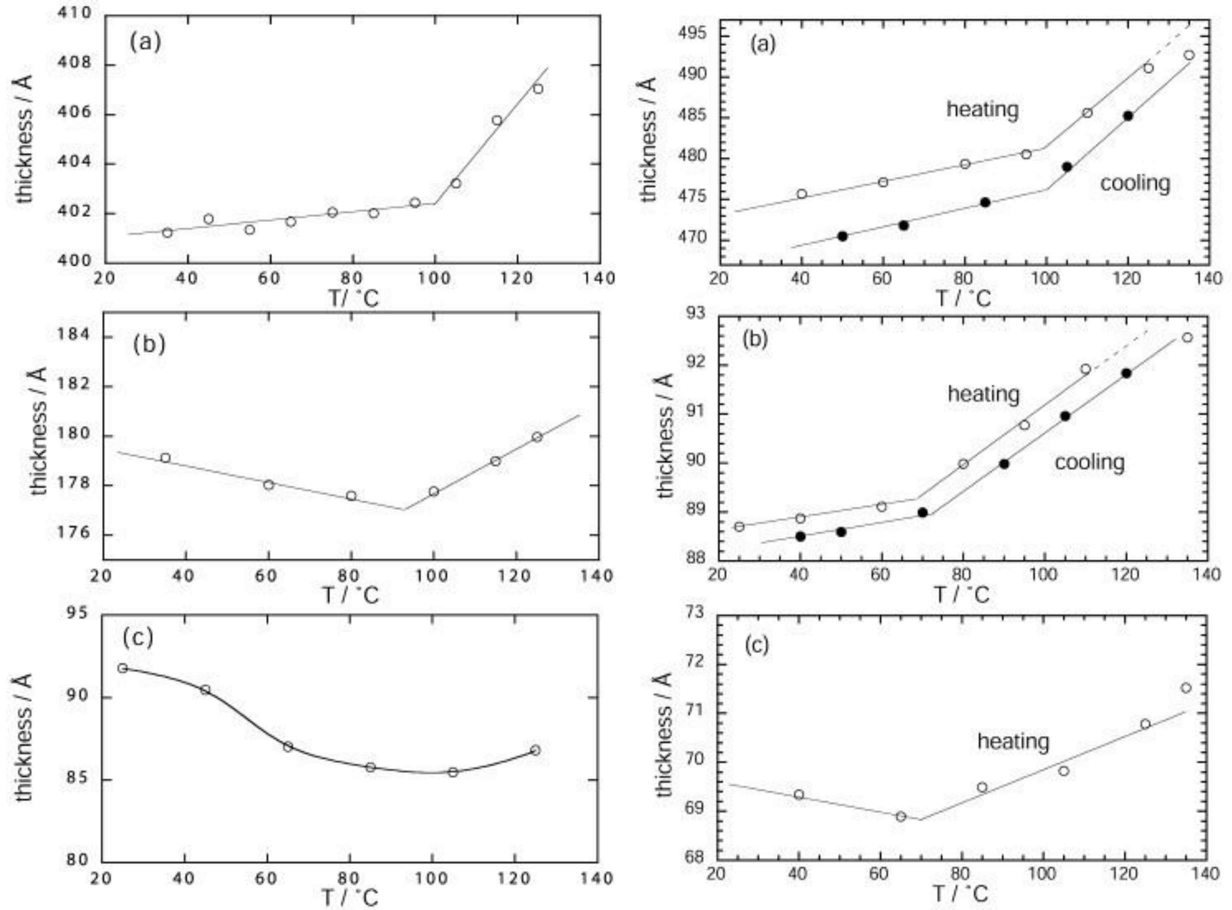

Figure 29. Temperature dependence of thickness of weakly annealed (left) and strongly annealed (right) deuterated polystyrene thin films with various values of initial thickness. For the strongly annealed experiment, measurements were done in heating and cooling process. [15]

From these experiment results, the negative thermal expansivity is observed for the thinner films. It is clear that further experiments are needed to explain this behavior.

Figure 30 shows the x-ray reflectivity results for the PS 9nm thick film.

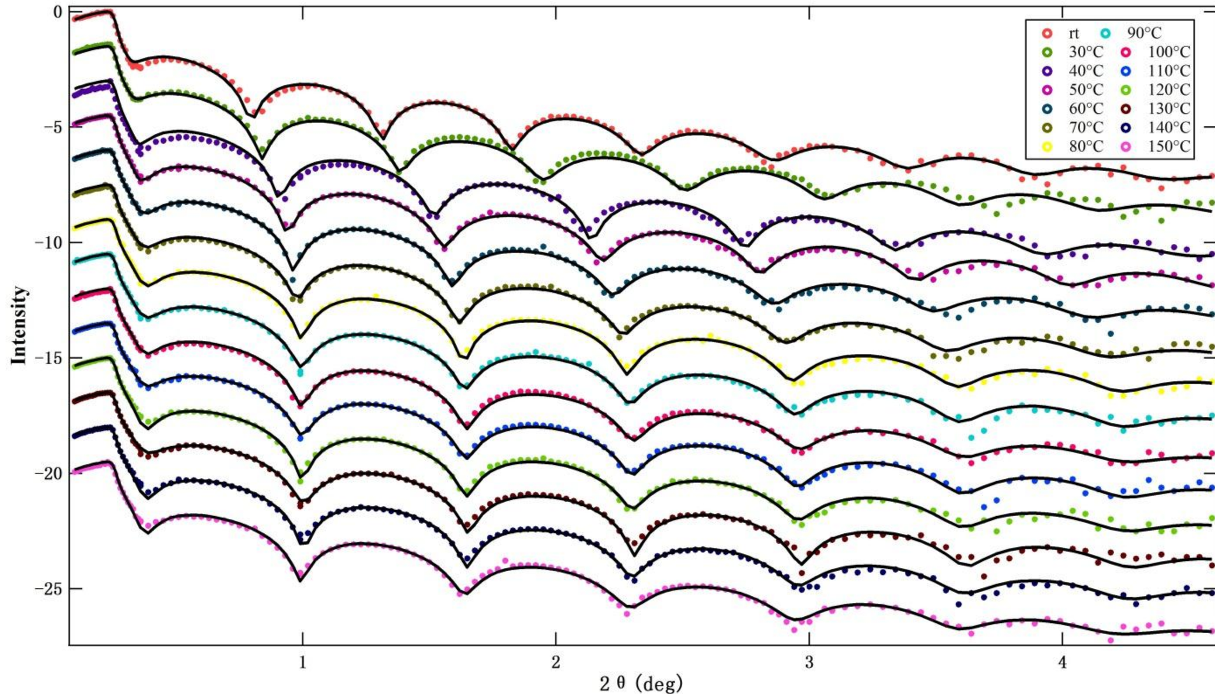

Figure 30. Specular reflectivity profiles and their corresponding modeled fits (solid lines) measured for PS (9nm in thickness, 150℃ for 24h annealed) with increasing temperature under vacuum

Table 7 summarizes the fitting results based on a three layer model.

Temperature(℃)	thickness(Å)	delta (×10^{-6})	Roughness(Å)
rt	96.46	1.17	3.51
30	90.01	1.10	3.20
40	82.31	1.18	5.00
50	80.36	1.18	3.55
60	78.70	1.16	3.56
70	77.40	1.12	4.90
80	76.66	1.15	3.68
90	76.40	1.12	4.55
100	76.04	1.13	5.10
110	76.15	1.10	4.62
120	76.12	1.21	4.11
130	75.77	1.21	4.00
140	76.03	1.21	3.86
150	76.44	1.22	4.28

Table 7. Thickness, delta and roughness for PS (9nm in thickness, 150℃ for 24h annealed) with increasing temperature under vacuum.

Figure 31 shows the thickness and delta values for PS (9nm in thickness, 150℃ for 24h annealed) as a function of temperature under vacuum.

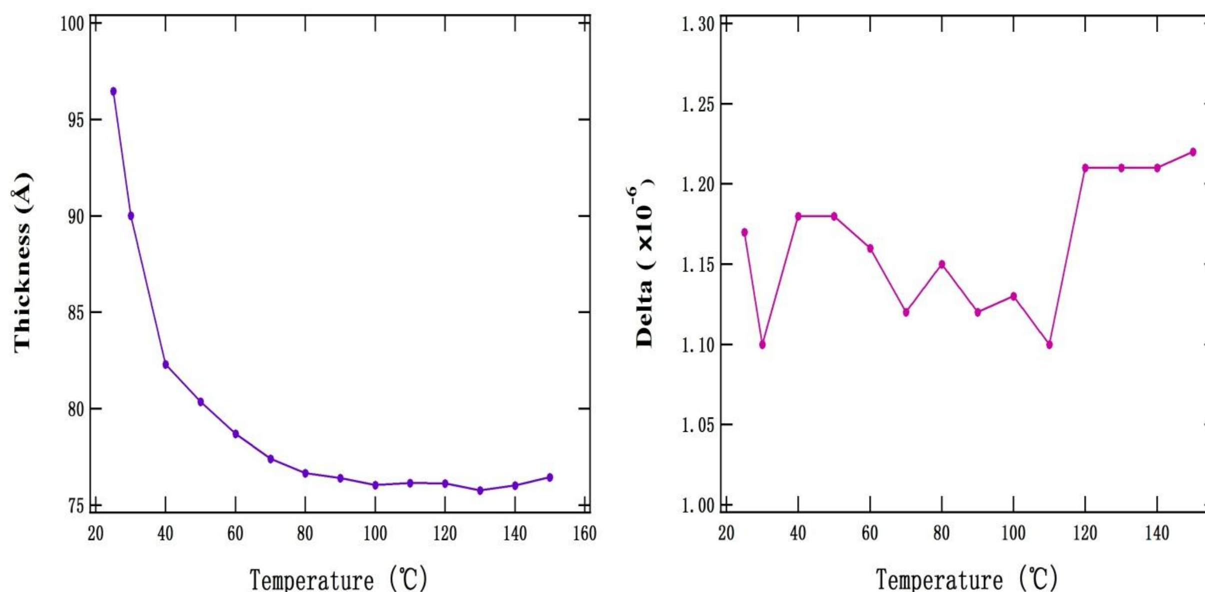

Figure 31. Thickness and delta for PS (M_w=290K, 9nm in thickness, 150℃-24h annealing) vs. temperature, measuring under vacuum.

From the observed and fitting profiles, we can see that the thickness decreased significantly from 30°C to 60°C, and then decreased slightly from 60°C to 90°C. After around 90°C we observed zero or quite small thermal expansivity. The trend is as same as 4nm PS thick film.

α (25°C-40°C) = $-7.86\times10^{-3}K^{-1}$

α (40°C-80°C) = $-1.8\times10^{-3}K^{-1}$

α (T>90°C)= 0

Figure 32 shows the XR profiles for the spin-cast PS film (50nm in thickness, 150°C for 24h annealing) as a function of temperature. The best-fits could be obtained by the four layer model (Si, SiO_2, top PS, and bottom PS layer).

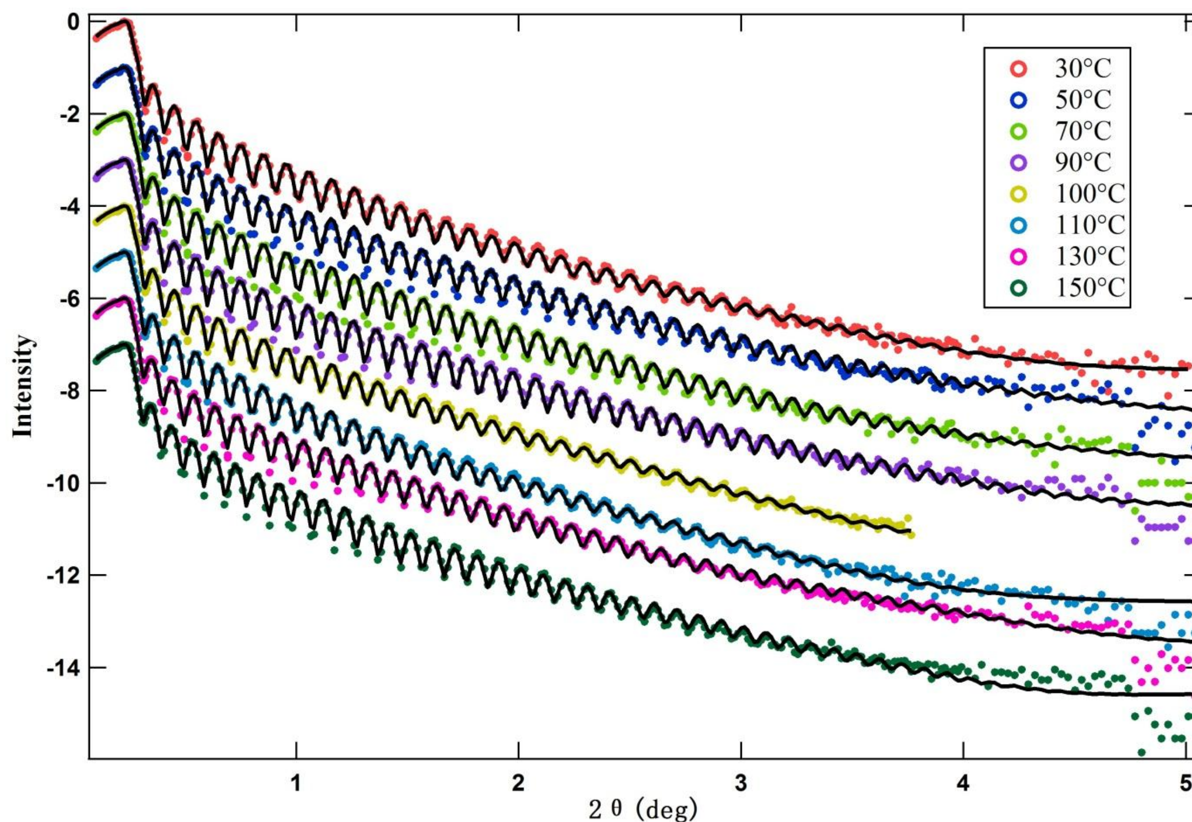

Figure 32. Specular reflectivity profiles and their corresponding modeled fits (solid lines) measured for PS (50nm in thickness, 150℃ for 24h annealed) under vacuum with varying temperature.

The fitting results are summarized in Table 8.

Temperature (℃)	Bottom layer thickness(Å)	Bottom layer delta ($\times 10^{-6}$)	Top layer thickness(Å)	Top layer delta ($\times 10^{-6}$)	Total thickness(Å)
30	15.957	1.2241	462.71	1.1495	478.7
50	15.432	1.25	464.73	1.15	480.2
70	16.012	1.25	462.78	1.16	478.8
90	16.073	1.2648	464.98	1.1741	481.1
100	16.464	1.2218	461.93	1.129	478.4
110	16.129	1.2454	464.78	1.1408	480.9
130	15.358	1.2561	475.74	1.1424	491.1
150	15.992	1.3086	480.74	1.1311	496.7
30 (after cooling)	16.464	1.2304	463.95	1.1536	480.42

Table 8. Thickness, delta and roughness for PS (50nm in thickness, 150℃ for 24h annealed) with increasing temperature under vacuum.

Measuring the sample back to 30℃ in vacuum condition after the heating experiment, we found that the sample has contracted back to its initial thickness, indicating the behavior is reversible. Figure 33 shows the bottom and top layer thickness values as a function of temperature.

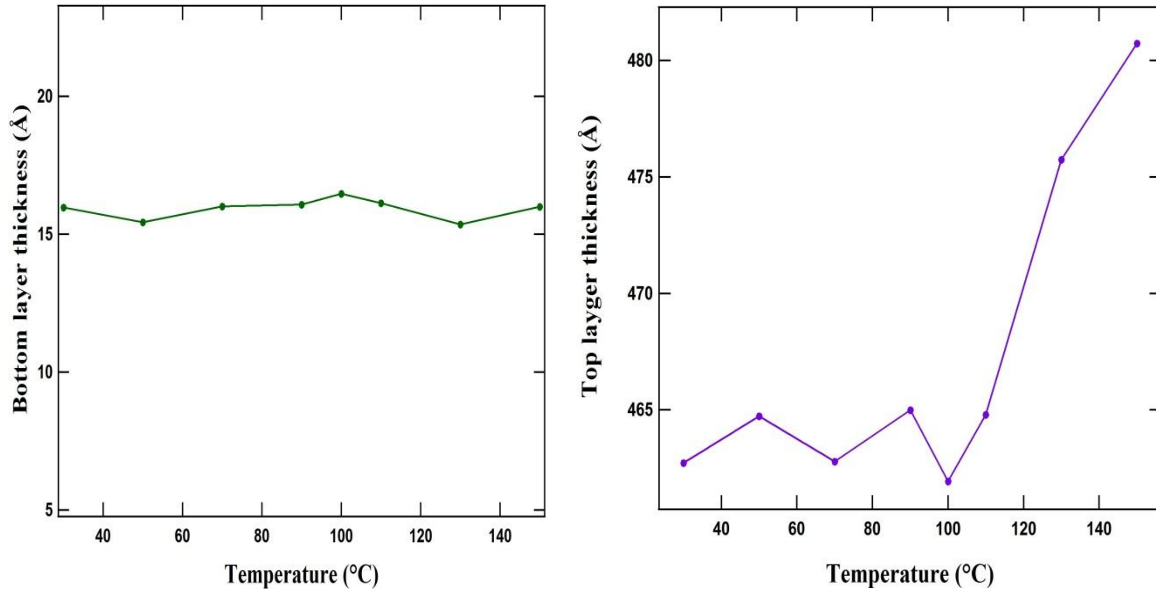

Figure 33. Thickness of bottom and top layer vs. Temperature.

From the figure 34, the thickness of the bottom layer doesn't change, i.e. zero thermal expansivity in the experimental temperature range. Namely, this layer corresponds to the dead layer. However, the thickness at the top layer has a significant increase at T>100℃. This is an indication of T_g.

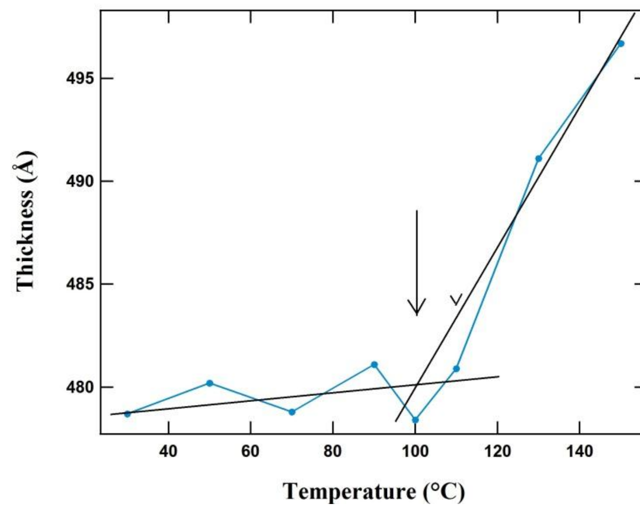

Figure 34. Total thickness vs. temperature.

The result of the thermal expansivity (a) are as followed:

α (30°C-110°C) = $5.744 \times 10^{-5} K^{-1}$

α (110°C-150°C) = $8.043 \times 10^{-4} K^{-1}$

These are in good agreement with the bulk PS.

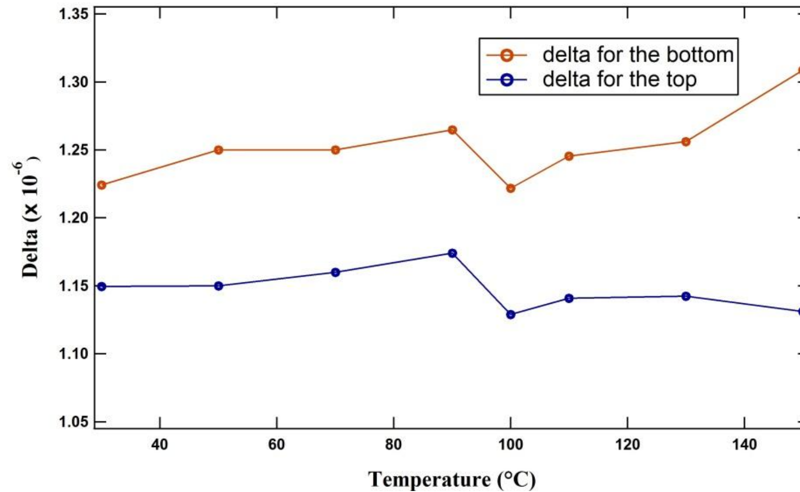

Figure 35. Delta for the bottom and top layer vs. temperature respectively.

We can see obviously that the delta at the bottom layer is larger than that of the top layer delta. The delta value of the bottom layer is consistent with that of the dead layer, as discussed before. It is obvious that the negative thermal expansion appears only in very thin films the thickness of 100Å.

Chapter 5 Conclusion

1. By using high temperature x-ray reflectivity experiments, we characterized the film structures of the adsorbed polystyrene layer onto silicon substrates, which could be obtained by intensive washing by toluene. We found that two hours annealing time at 150℃ is enough to obtain the equilibrium thickness of the adsorbed layer. This behavior is true even when we used the different concentration of PS/toluene solution (2.5wt% and 0.2wt%). The final thickness was 63Å for the lower concentration, while that for the higher concentration was 93Å.

2. When we further immersed the adsorbed layer in toluene, we found that the thickness of the adsorbed layer decrease with the immersing time. The thickness became 40Å after 5 month. This thickness is in good agreement with Gin's experimental result by using $ScCO_2$.

3. We found the thickness of the adsorbed layer decreased with increasing temperature, similar trend was observed for spin-cast PS thin films with 4nm and 9nm in thickness, while the 50nm thick film showed the positive thermal expansion coefficient. Further studies are needed to explain this anomalous thermal expansion coefficient of the adsorbed layer as well as 4nm, 9nm thick films.

References

[1] C. J. Drury, C. M. Hart, Appl. Phys. Lett. **73**, 108 (1998)
[2] J. L. Keddie, R. A. Jones, and R. A. Cory, Europhys. Lett. 27, 59 (1994).
[3] J. L. Keddie, R. A. Jones, and R. A. Cory, Faraday Discuss. **98**, 219 (1994).
[4] S. Kawana and R. A. L. Jones, Phys. Rev. E **63**, 021501 (2001).
[5] T. Miyazaki, K. Nishida, and T. Kanaya, Phys. Rev. E **69**, 061803 (2004).
[6] W. J. Orts et al., Phys. Rev. Lett. **71**, 867 (1993).
[7] T. Miyazaki, K. Nishida, and T. Kanaya, Phys. Rev. E **69**, 022801 (2004).
[8] G. Reiter et al., Nature Mater. **4**, 754 (2005).
[9] J. L. Keddie, R. A. L. Jones, and R. A. Cory, Faraday Discuss. 98, 219 (1994).
[10] S. Kawana and R. A. L Jones, Phys. Rev. E **63**, 21501 (2001).
[11] N. Satomi, A. Takahara, and T. Kajiyama, Macromolecules **32**, 4474 (1999).
[12] N. Satomi, K. Tanaka, A. Takahara, T. Kajiyama, T. Ishizone, and S. Nakahama, Macromolecules **34**, 8761 (2001).
[13] H. Fischer, Macromolecules **35**, 3592 (2002).
[14] A. D. Schwab, D. G. Agra, J. H. Kim, S. Kumar, and A. Dhinojwala, Macromolecules **33**, 4903 (2000).
[15] T. Kanaya, T. Miyazaki, H. Watanabe, K. Nishida, H. Yamano, S. Tasaki, and D. B. Bucknall, Polymer **44**, 3769 (2003).
[16] W. J. Orts, J. H. van Zanten, W.-l. Wu, and S. K. Satija, Phys. Rev. Lett. **71**, 867 (1993).
[17] K. Fukao and Y.Miyamoto, Phys. Rev. E **61**, 1743 (2000).
[18] A. Serghei, M. Tress, and F. Kremer, Macromolecules 39, 9385 (2006).
[19] A. Serghei, M. Tress, and F.Kremer, J. Chem. Phys. **131**, 154904 (2009).
[20] K. Tanaka, Y. Tateishi, Y. Okada, T. Nagamura, M. Doi, and H. Morita, J. Phys. Chem. B **113**, 4571 (2009).
[21] R. Inoue, T. Kanaya. Phys. Rev. E **84**, 031802 (2011)
[22] R. Inoue, K. Kawashima, K. Matsui, T. Kanaya, K. Nishida, G. Matsuba, and M. Hino, Phys. Rev. E **83**, 021801 (2011).
[23] C. J. Ellison and J. M. Torkelson, Nat. Mater. **2**, 695 (2003).
[24] K. Akabori, K. Tanaka, T. Nagamura, A. Takahara, and T. Kajiyama, Macromolecules **38**, 9735 (2005).
[25] W. E.Wallace, J. H. van Zanten, andW. L.Wu, Phys. Rev. E **52**, R3329 (1995).
[26] D. Kawaguchi, K. Tanaka, T. Kajiyama, A. Takahara, and S. Tasaki, Macromolecules **36**, 1235 (2003).
[27] T.Q. Nguyen, I. Martini, J. Liu, and B. J. Schwartz, J. Phys. Chem. B **104**, 237 (2000).
[28] Wallace, W. E.; van Zanten, J. H.; Wu, W. L. Phys. Rev. E **52**, R3329 (1995)
[29] Keddie, J. L.; Jones, R. A. L.; Cory, R. A. Europhys. Lett. **27**, 59 (1994)
[30] H. W. Hu and S. Granick, Science **258**, 1339 (1992)
[31] J. L. Keddie, R. A. L. Jones, and R. A. Cory, Europhys. Lett. **17**, 59 (1994)

[32] W. E. Wallace, J. H. van Zanten, Phys. Rev. E **52**, 4 (1995)
[33] C. Redon, F. Brochard-Wyart, and F. Rondelez, Phys. Rev. Lett. 66, 715 (1991).
[34] R. Gunter. Phys. Rev. Lett. 87. 186101 (2001)
[35] S. A. Safran and J. Klein, J. Phys. II (France) 3, 749 (1993).
[36] D. J. Srolovitz and S. A. Safran, J. Appl. Phys. 60, 247 (1986).
[37] D. J. Srolovitz and S. A. Safran, J. Appl. Phys. 60, 255 (1986).
[38] A. Sharma, J. Colloid Interface Sci. 199, 212 (1998).
[39] A. Oron and S. G. Bankoff, J. Colloid Interface Sci. 218, 152 (1999).